Hafnium isotopic variations in volcanic rocks from the Caribbean Large Igneous Province and Galápagos hot spot tracks

J. Geldmacher

Baylor Brooks Institute for Isotope Geochemistry, San Diego State University, 5500 Campanile Drive, San Diego, California 92182, USA

Now at Geomar Forschungszentrum, Wischhofstrasse 1–3, 24148 Kiel, Germany (jgeldmacher@geomar.de)

B. B. Hanan

Baylor Brooks Institute for Isotope Geochemistry, San Diego State University, 5500 Campanile Drive, San Diego, California 92182, USA (bhanan@mail.sdsu.edu)

J. Blichert-Toft

Laboratoire des Sciences de la Terre, Ecole Normale Supérieure de Lyon, 69364 Lyon Cedex 7, France (jblicher@ens–lyon.fr)

K. Harpp

Department of Geology, Colgate University, Hamilton, New York 13346, USA (kharpp@mail.colgate.edu)

K. Hoernle and F. Hauff

Geomar Forschungszentrum, Wischhofstrasse 1–3, 24148 Kiel, Germany (khoernle@geomar.de; fhauff@geomar.de)

R. Werner

Tethys Geoconsulting GmbH, c/o Geomar Wischhofstrasse 1–3, 24148 Kiel, Germany (rwerner@geomar.de)

A. C. Kerr

Department of Earth Sciences, Cardiff University, P.O. Box 914, Cardiff, CF10 3YE, UK (kerra@cf.ac.uk)

[1] We report Hf isotope compositions of 79 lavas that record the early (∼5–95 Ma) history of the Galápagos plume volcanism. These include lavas from the Caribbean Large Igneous Province (CLIP; ∼95–70 Ma), the accreted Galápagos paleo-hot spot track terranes (54–65 Ma) of Costa Rica (Quepos, Osa and Burica igneous complexes), and the Galápagos hot spot tracks (<20 Ma) located on the Pacific seafloor (Cocos, Carnegie, Malpelo, and Coiba Ridges and associated seamounts). These samples have previously been well characterized in terms of major and trace elements, Sr-Nd-Pb isotopes and Ar/Ar ages. As a result of the relative immobility of the high field strength and rare earth elements during syn- and post-emplacement hydrothermal activity and low-temperature alteration, combined Lu-Hf and Sm-Nd isotope systematics, when used in conjunction with Pb isotopes, provide a particular powerful tool, for evaluating the source compositions of ancient and submarine lavas. The combined Nd-Hf isotope data suggest that three of the isotopically distinct source components found today in the Galápagos Islands (the Floreana-like southern component, the Fernandina-like central component, and the depleted Genovesa-like eastern component) were present in the CLIP already by 95–70 Ma. The fourth Pinta-like northern component is first recorded at about 83–85 Ma by volcanism taking place during the transition from the plume head/CLIP to plume tail stage and has then been present in the hot spot track continuously thereafter. The identification of the unique northern and southern Galápagos Plume Hf-Nd-Pb isotope

source signatures within the CLIP and the oldest hot spot track lavas provides direct evidence that the CLIP represents the plume head stage of the Galápagos hot spot. Hafnium isotopes are consistent with the possibility that two types of sediment components may have contributed to the Hf, Nd and Pb isotope compositions of the Galápagos plume lavas. One component, characterized by $\Delta^{207}Pb/^{204}Pb \approx 0$ and high positive $\Delta\varepsilon Hf$ has an isotope signature indicative of relatively recently recycled pelagic sediment, a signature typical of the southern Galápagos island Floreana. The other component has an EM like isotopic composition resembling modern seafloor sediments with positive $\Delta^{207}Pb/^{204}Pb$ and lower $\Delta\varepsilon Hf$, a signature typical of the northern Galápagos island Pinta.

1. Introduction

[2] The Caribbean Large Igneous Province (CLIP) consists of the Caribbean oceanic plateau and associated magmatic terranes along the Pacific coast of central America and western Colombia (Figure 1). On the basis of plate tectonic reconstructions [e.g., *Duncan and Hargraves*, 1984; *Pindel and Barrett*, 1990] and geochronological data [*Hauff et al.*, 1997; *Sinton et al.*, 1997; *Kerr et al.*, 1997b; *Hauff et al.*, 2000a], the oceanic flood basalts of the CLIP are interpreted to mark the initiation of the Galápagos hot spot at $\sim$ 90 Ma with voluminous magmatism generated from the starting plume head [*Richards et al.*, 1989].

[3] Geochemical data from present-day Galápagos Islands and submarine volcanic platform lavas define an east facing horseshoe pattern of depleted geochemical signatures at the center of the archipelago and more enriched signatures along the periphery [*White and Hofmann*, 1978; *Geist et al.*, 1988; *White et al.*, 1993; *Harpp and White*, 2001; *Blichert-Toft and White*, 2001]. Four distinct isotopic end-members are called upon to account for the variations observed in the Sr, Nd, Hf, Pb, and He isotope data of the Galápagos lavas [*Harpp and White*, 2001; *Blichert-Toft and White*, 2001]. Three

of the end-members have enriched radiogenic isotope signatures and are geographically distributed from northwest to southeast [*Hoernle et al.*, 2000]. Their characteristic signatures are represented by lavas from the islands of Pinta, Fernandina and Floreana, respectively [*Blichert-Toft and White*, 2001]. The remaining end-member is a relatively depleted component (e.g., represented by Genovesa), indistinguishable from the regular depleted asthenosphere MORB source, that dominates the eastern Galápagos Islands [*Harpp and White*, 2001; *Blichert-Toft and White*, 2001]. The mixing interaction between the end-members is reflected by a complex geochemical pattern across the Galápagos platform that *Hoernle et al.* [2000] interpreted to define four spatially distinct geographic domains for the archipelago and the Cocos Ridge paleo-Galápagos plume track (Figure 2). The southern domain (Floreana Island), the central domain (Fernandina and large parts of Isabela Island) and the northern domain (Pinta, Wolf and Darwin islands) form a horseshoe-shaped pattern of enriched isotope compositions around the more depleted eastern domain (Genovesa, Santa Cruz, San Cristobal). Studies of basalts from the submarine Cocos, Carnegie, Malpelo and Coiba Ridges forming the Galápagos hot
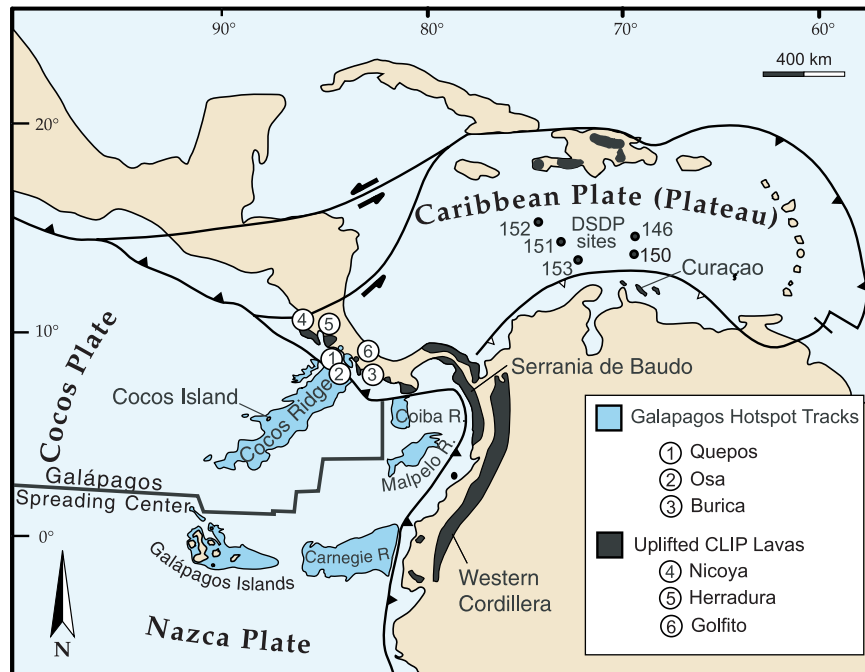
Figure 1. The Caribbean Large Igneous Province and Panáma Basin (modified after *Kerr et al.* [1997a] and *Hauff et al.* [1997]).

spot track indicate that the present geographic pattern of geochemical variation of the plume components has persisted for at least 17 million years [*Hoernle et al.*, 2000, 2002a; R. Werner, K. Hoernle, U. Barckhausen, and F. Hauff, The Geodynamic Evolution of the Galápagos System (Central East Pacific) over the past 20 m. y.: Constrains from Morphology, Geochemistry, and Magnetic Signatures, manuscript submitted to *Geochemistry Geophysics Geosystems*, 2003, hereinafter referred to as Werner et al., submitted manuscript, 2003]. The origin of the Galápagos source components and the apparent spatial distribution of the Galápagos domains are both controversial issues. It is currently debated whether these observations are related to heterogeneity within the plume as it impinges on the base of the lithosphere [e.g., *Hauff et al.*, 2000a, 2000b; *Hoernle et al.*, 2000; *Kerr et al.*, 2002] or in part to plume interaction with the upper mantle MORB source [e.g., *Harpp and White*, 2001; *Blichert-Toft and White*, 2001].

[4] To constrain further the mantle mixing processes of the Galápagos Plume through time and to explore the nature and origin of the observed

mantle geochemical signatures, we here report 79 new Hf isotope analyses of volcanic rocks from widespread locations within the CLIP and from the Cocos, Malpelo, Carnegie and Coiba submarine ridges of the Galápagos hot spot track. The immobility of the refractory Lu-Hf system during seafloor alteration processes provides an especially power-
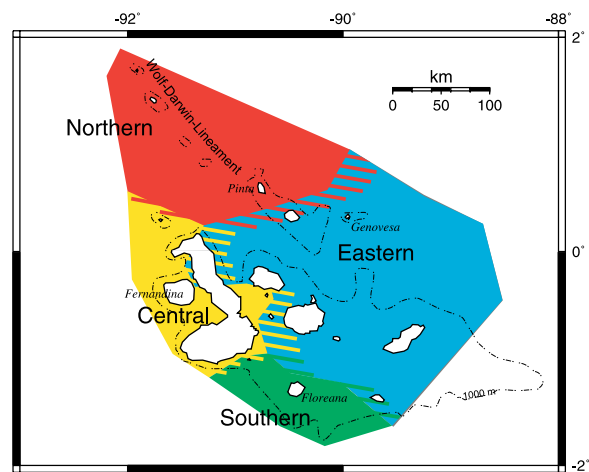

Figure 2. The Galápagos archipelago and distribution of the four isotopically defined geographic domains (modified from *Hoernle et al.* [2000] taking into consideration the Galápagos submarine platform isotope data from *Harpp and White* [2001]).

ful tool for evaluating the source compositions of ancient lavas erupted in a submarine environment. Hafnium combined with Nd and Pb isotope ratios therefore allow us to gain new insights into the components and hence sources involved in the earlier history of the Galápagos hot spot. The samples analyzed here for Hf isotope compositions have been previously analyzed for Pb, Sr, and Nd isotope compositions and trace element abundances [*Hoernle et al.*, 2000; *Hauff et al.*, 2000a, 2000b; Werner et al., submitted manuscript, 2003].

2. Geodynamic Background and Ages of the Sampling Sites

[5] In the following, we briefly summarize the tectonic and geologic history of the CLIP and Galápagos region. After the formation of the CLIP oceanic plateau in the equatorial Pacific northeastward plate motion of the Farallon Plate resulted in its collision with the Greater Antilles Arc, causing a reversal in polarity of subduction in the Greater Antilles Arc and initiation of subduction on the western margin of the CLIP. The reversal in polarity allowed the plateau to insert itself between the converging Americas during the Late Cretaceous to early Tertiary [e.g., *Duncan and Hargraves*, 1984; *Hauff et al.*, 2000a; *Hoernle et al.*, 2002a]. Age dating indicates that the majority of CLIP lavas erupted during the period between 95–70 Ma, possibly with multiple pulses of magmatism [*Kerr et al.*, 1997b; *Sinton et al.*, 1998; *Hauff et al.*, 2000a].

[6] The oldest CLIP areas analyzed for Hf isotopes in this study are the tholeiitic Nicoya and Herradura complexes in northern Costa Rica (Figure 1) with $^{40}Ar/^{39}Ar$ ages between 83–95 Ma [*Sinton et al.*, 1997; *Hauff et al.*, 2000a]. There are no radiometric age data for the Golfito terrane in southern Costa Rica, but stratigraphic relationships suggest formation of these magmatic rocks before 74 Ma [*Hauff et al.*, 2000a]. Age determinations on DSDP-cores from sites 150 and 146 drilled into the upper lava succession of the intact Caribbean Plateau during DSDP Leg 15 (see Figure 1) yield ages between 90 and 94 Ma [*Sinton et al.*, 1998]. Lavas at DSDP sites 151 (~83–85 Ma) [*Donnelly et al.*, 1973] and

152 (75 Ma) [*Sinton et al.*, 1998] are younger. $^{40}Ar/^{39}Ar$ ages of 72–77 Ma are reported for the thrust fault-bounded Serranía de Baudó terrane in western Colombia [*Kerr et al.*, 1997b]. Among the Western Cordillera lavas analyzed in this study, sample PAN 6 from the central region has yielded an $^{40}Ar/^{39}Ar$ age of 92 Ma [*Sinton et al.*, 1998]. Field relationships and intercalated sediments suggest a similar age for most of the Western Cordillera magmas [*Kerr et al.*, 1997b]. However, $^{40}Ar/^{39}Ar$ ages of 76 Ma for lavas in the northern region of the Cordilleras [*Sinton et al.*, 1998] suggest the Western Cordilleras do not represent a complex formed in a single magmatic episode. The bulk of the Curaçao lavas accumulated during a short time span between 88–89 Ma [*Sinton et al.*, 1998].

[7] Considerably younger $^{40}Ar/^{39}Ar$ ages of 54–65 Ma are reported for the Quepos, Osa and Burica terranes of central Costa Rica [*Sinton et al.*, 1997; *Hauff et al.*, 2000a; *Hoernle et al.*, 2002a]. Petrological and volcanological evidence (e.g., partly subaerial volcanism at Quepos) suggest these complexes were parts of former ocean islands and aseismic ridges formed above the tail of the Galápagos plume after the plume head-generated oceanic plateau drifted off toward the northeast. Therefore Quepos, Osa and Burica, as well as igneous terranes accreted in western Panama, are thought to represent the oldest parts of the Galápagos hot spot tracks, which were accreted to the CLIP after the insertion of the plateau between North and South America and the onset of subduction beneath its western margins at 66–71 Ma [*Hoernle et al.*, 2002a]. High $^{3}He/^{4}He$ signatures of Quepos picritic lavas (11.4–11.7 R/R$_A$) [*Hauff et al.*, 2000b] are comparable to the He isotope compositions characteristic of the present-day western Galápagos islands [*Graham et al.*, 1993].

[8] The best-studied submarine part of the Galápagos hot spot tracks is the northeastern end of the Cocos Ridge off the Central American coast (Figure 3) with an age of 13.0–14.5 Ma [*Werner et al.*, 1999; *Hoernle et al.*, 2000]. In addition to the Cocos Ridge, the Malpelo, Carnegie and Coiba Ridges in the Panama Basin may also form parts of the Galápagos hot spot tracks [*Wilson and Hey*,
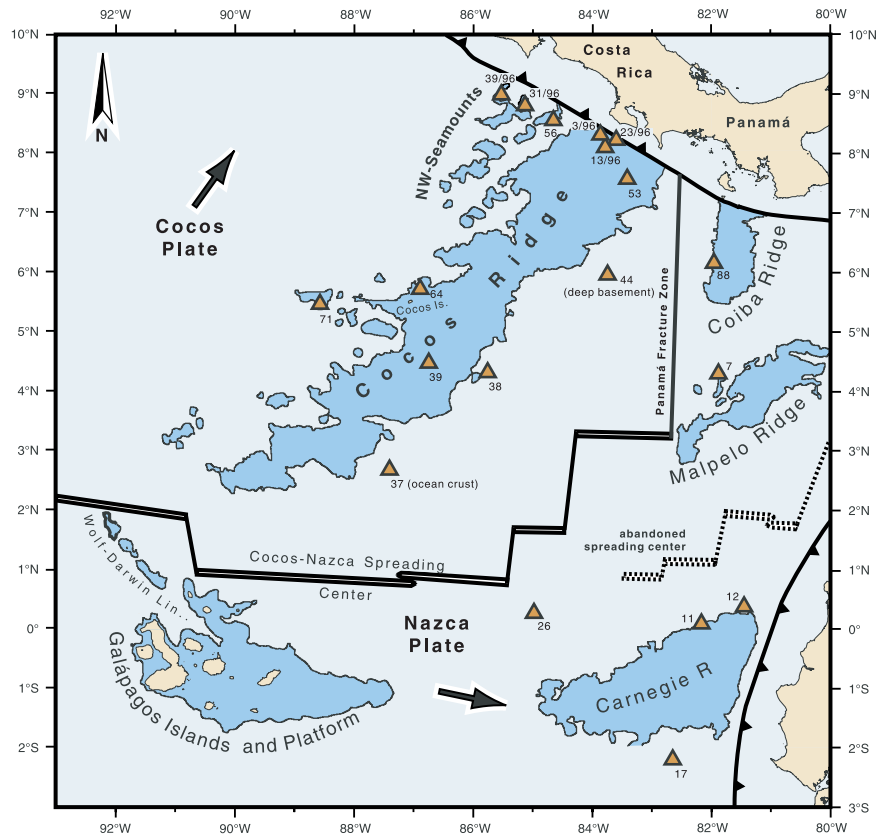
Figure 3. Submarine ridges of the Panáma basin (modified after Werner et al., submitted manuscript, 2003). For clarity only −2000 m contour is shown. Triangles mark the sampling sites of the submarine lavas analyzed in this study (numbers refer to samples in Table 1).

1995; Werner et al., submitted manuscript, 2003]. It has been proposed that the Farallon plate split into the northeasterly migrating Cocos and the easterly migrating Nazca plates at about 25 Ma [*Handschumacher*, 1976]. The aseismic Malpelo and Carnegie Ridges were formed when the Galápagos hot spot was ridge-centered beneath the Cocos/Nazca spreading center [*Barckhausen et al.*, 2001]. Relocation of the spreading center and initiation of the Panamá Fracture Zone presently located at 83°W ended spreading east of the fracture zone and cut off the Malpelo and Coiba ridge from its younger, western end, which became the Cocos Ridge. Around 15 Ma the spreading center was located south of the hot spot [*Werner et al.*, 1999] and only the Cocos Ridge formed while production of the Carnegie Ridge ended. Another ridge shift between 3–5 Ma gradually moved the spreading center to the north of the hot spot and resulted in extinction of the Cocos Ridge and the

creation of the Galápagos archipelago [Werner et al., submitted manuscript, 2003]. The origin and tectonic relationships of the Coiba Ridge is less well understood. It may be exclusively a tectonic feature and not part of the Galápagos hot spot track.

3. Analytical Methods and Results

[9] Hafnium isotope analyses were carried out on rock powders prepared from carefully hand-picked whole rock chips and fresh glass shards. Description of sampling and sample preparation are given in Werner et al. [submitted manuscript, 2003] for the submarine lavas and in *Hauff et al.* [1997, 2000b] for the CLIP samples. Hafnium was separated at San Diego State University following the two-column procedure outlined in *Blichert-Toft et al.* [1997]. Hafnium isotope ratios were measured by multiple collector magnetic sector inductively

coupled plasma mass spectrometry (MC-ICP-MS) using the "VG Plasma 54" at Ecole Normale Supérieure in Lyon. During the period of analysis of the present samples (four consecutive days), replicate measurements of the JMC-475 Hf standard averaged 0.28216 ± 0.00001 (2σ, n = 38) for $^{176}Hf/^{177}Hf$. The standard was run repeatedly every two to three samples to verify machine performance. The average in-run precision on sample $^{176}Hf/^{177}Hf$ was better than ± 0.000009 (2σ). $^{176}Hf/^{177}Hf$ was normalized for instrumental mass bias relative to $^{179}Hf/^{177}Hf = 0.7325$. Measured and initial Hf isotope ratios are presented in Tables 1 and 2. The same samples have been previously analyzed for Nd, Sr and Pb isotopes and trace elements: data for the submarine ridge samples are presented in *Hoernle et al.* [2000] and Werner et al. [submitted manuscript, 2003] whereas data for the CLIP samples can be found in *Hauff et al.* [2000a, 2000b].

[10] To compare the isotopic signatures for the Cocos, Carnegie, Malpelo and Coiba submarine and CLIP lavas to those of present-day Galápagos data, the initial isotope ratios were calculated from the measured data and then projected forward in time to the isotope composition they would have today. For the initial ratio calculations we used the parent-daughter trace element concentration and age data from, respectively, *Hauff et al.* [2000a, 2000b] and from *Hoernle et al.* [2000] and Werner et al. [submitted manuscript, 2003] for the CLIP and submarine lavas. The initial ratios were then projected to present-day values by adding the radiogenic in-growth according to their age and an assumed parent-daughter ratio as formulated by *Sun and McDonough* [1989] for the oceanic island basalt (OIB) mantle source. In principle, the calculated initial isotope ratios are susceptible to possible inaccuracy because of potential post crystallization redistribution due to seawater alteration, weathering or metamorphic effects. *Hauff et al.* [2000b] have discussed the potential impact of secondary effects on the Nd, Sr, and Pb isotopes and have argued that the Pb and Nd isotopes were the least affected. Therefore we have not projected the Sr isotopes. Details of the CLIP Sr isotopes can be found in *Hauff et al.* [2000b]. For Hf isotope ratios, however,

we estimate such secondary effects to be either absent or minimal due to the refractory character of both Lu and Hf and the effort made in the present study to only select samples for Hf isotope analysis that showed minimal secondary effects.

3.1. Cocos, Carnegie, Malpelo, and Coiba Ridges

[11] With respect to the global Nd-Hf isotope mantle array (Figure 4a), $^{176}Hf/^{177}Hf$ shows the expected overall positive correlation with $^{143}Nd/^{144}Nd$. Most of the submarine aseismic ridge data are from the eastern end of Cocos Ridge, dredged in a profile roughly perpendicular to the ridge axis and plate motion (see sample sites in Figure 3). The data are grouped with respect to their geographic locations along the ridge axis (Table 1). The εHf ratios of Cocos Ridge samples range from the most extreme value of +11.9 for a lava dredged in a deep valley cutting the ridge basement to less radiogenic values falling between +4.2 and +9.2 for rocks obtained from the northern flank of the ridge (Figure 4b). Dredged volcanic rocks from the central and southern segments of the Cocos Ridge show intermediate Hf isotope compositions. Most of the samples from the Malpelo, Carnegie and Coiba Ridges show similar intermediate εHf. Sample 26TVG-1 from a seamount on the northern flank of Carnegie Ridge has the most depleted composition of all measured ridge samples with εHf = +12.5. Also shown is the Hf isotopic composition of a Pacific MORB sample (37 DR-1) dredged SE of Cocos Ridge.

[12] In Nd-Hf-Pb isotope variation diagrams, Cocos Ridge lavas form fields that also correspond to spatially distinct geographic groups. These fields show the same relative spatial and isotopic characteristics as the present-day Galápagos end-members and domains. This is most clearly seen in plots of Hf versus Pb isotopes (Figures 5a, 5b, and 5c). In the εHf versus $^{206}Pb/^{204}Pb$ and $^{207}Pb/^{204}Pb$ diagrams, the different trends for the individual Cocos Ridge regions radiate from the intermediate Fernandina-like central Galápagos domain composition toward the Floreana-like southern, Pinta-like northern and Genovesa-like eastern domains. The northern and southern Cocos regions are relatively enriched in

Table 1. Sample Localities and Hf Isotope Compositions (±2σ) of Submarine Ridges in the Panama Basin[a]

Sample	Coordinates	Age	Lu	Hf	U	Th	Pb	$^{176}Hf/^{177}Hf_m$	ε Hf	$^{176}Lu/^{177}Hf$	$^{176}Hf/^{177}Hf_{in}$	$^{176}Hf/^{177}Hf_t$	ε Hf$_t$
Northern Cocos Ridge													
39/96 Co (NW Seamount)	9°02, 7'N; 85°28, 7'W	14	0.57[b]	8.51[b]	1.39[b]	4.72[b]	2.75[b]	0.283032 (8)	9.2	0.0096	0.283029	0.283030	9.1
31/96 Co (NW Seamount)	8°47, 7'N; 85°12, 5'W	14	0.28[b]	5.85[b]	1.08[b]	3.86[b]	2.53[b]	0.282940 (10)	5.9	0.0069	0.282938	0.282940	5.9
56/96 Co (NW Seamount)	8°39, 9'N; 84°39, 4'W	14	0.54[b]	10.0[b]	3.34[b]	6.20[b]	2.47[b]	0.282890 (8)	4.2	0.0077	0.282887	0.282889	4.1
3/96 Co (north. ridge flank)	8°15, 5'N; 83°53, 2'W	14	0.32[b]	5.89[b]	1.24[b]	5.19[b]	2.22[b]	0.283010 (8)	8.4	0.0078	0.283008	0.283009	8.4
64 DR-1 Cocos Island	5°45, 66'N; 86°54, 08'W	2[d]	0.42	5.86	1.29	5.62	2.14	0.283021 (6)	8.8	0.0103	0.283021	0.283021	8.8
71DR-1 Cocos Seamount	5°30, 96'N; 88°34, 79'W	4–6[c]	0.57	9.05	1.31	1.37	3.20	0.283012 (8)	8.5	0.0090	0.283011	0.283012	8.5
Central Cocos Ridge													
13/96 Co	8°07, 0'N; 83°50, 0'W	14	0.45[b]	3.22[b]	0.54[b]	0.88[b]	0.68[b]	0.283086 (9)	11.1	0.0202	0.283080	0.283082	10.9
23/96 Co	8°17, 5'N; 83°43, 4'W	14	0.58[b]	3.96[b]	1.97[b]	1.32[b]	0.61[b]	0.283092 (11)	11.3	0.0211	0.283086	0.283087	11.1
Southern Cocos Ridge													
63/96 Co	8°13, 8'N; 83°30, 6'W	14	1.53[b]	5.22[b]	1.21[b]	1.72[b]	0.76[b]	0.283092 (10)	11.3	0.0421	0.283080	0.283082	10.9
25/96 Co	8°12, 0'N; 83°29, 5'W	14	0.30[b]	2.05[b]	0.16[b]	0.53[b]	0.32[b]	0.283077 (11)	10.8	0.0209	0.283071	0.283073	10.6
39DR-2	4°30, 84'N; 86°46, 23'W	6[c]	0.40	3.69	1.96	1.11	0.78	0.283088 (10)	11.2	0.0155	0.283086	0.283087	11.1
53DR-1	7°36, 24'N; 83°25, 21'W	≥12[c]	0.53	3.73	1.19	1.22	0.61	0.283072 (7)	10.6	0.0204	0.283067	0.283069	10.5
38DR-12	4°21, 59'N; 85°47, 05'W	6[c]	0.32	4.20	1.28	5.27	2.01	0.283014 (11)	8.5	0.0109	0.283013	0.283013	8.5
Deep Basement, Cocos Ridge													
44 DR-14	5°58, 10'N; 83°40, 03'W	11[c]	0.38	1.40	0.05	0.09	0.29	0.283107 (9)	11.9	0.0389	0.283097	0.283098	11.5
Malpelo Ridge													
7 DR-1, NW margin	4°19, 92'N; 81°52, 48'W	14[c]	0.37	2.54	0.23	0.94	1.21	0.283107 (7)	11.8	0.0209	0.283101	0.283102	11.7
Carnegie Ridge													
11DR-1, N margin	0°03, 33'N; 82°07, 34'W	15[c]	0.34	2.07	2.07	0.34	0.37	0.283067 (8)	10.4	0.0235	0.283060	0.283062	10.3
12 DR-1, N margin	0°23, 89'N; 81°27, 18'W	20[c]	0.37	2.20	0.23	0.65	0.48	0.283092 (9)	11.3	0.0241	0.283083	0.283085	11.1
17 TVG-1, S margin	2°09, 83'S; 82°36, 64'W	15[c]	0.23	0.70	0.03	0.12	4.80	0.283048 (12)	9.7	0.0471	0.283034	0.283036	9.3
26 TVG-1, N seamount	0°18, 01'N; 84°58, 54'W	≥8[c]	0.43	2.65	1.20	0.41	0.60	0.283125 (7)	12.5	0.0233	0.283122	0.283122	12.4
Coiba Ridge													
88 DR-1, W scarp	6°12, 27'N; 81°56, 93'W	≥14[c]	0.61	6.22	0.92	2.55	1.64	0.283077 (11)	10.8	0.0141	0.283073	0.283071	10.7
MORB (SE of Cocos Ridge)													
37 DR-1	2°35, 32'N; 87°28, 92'W	3–5[c]	0.43	1.47	0.03	0.12	0.17	0.283171 (10)	14.1	0.0419	0.283168	0.283168	14.0

[a] εHf calculated relative to the chondritic value of 0.282772. Values projected for today's isotope composition of the mantle source (t) using their initial isotopic composition and age and the parent/daughter ratios for OIB's from *Sun and McDonough* [1989]. For Nd and Pb isotope data of these samples see *Hoernle et al.* [2000] and *Werner et al.* (submitted manuscript, 2003).

[b] Trace element concentrations from *Hoernle et al.* [2000].

[c] Assumed ages based on magnetic data, plate velocities, and age dating on corresponding samples (see *Werner et al.* (submitted manuscript, 2003) for references). All other ages based on *Werner et al.* [1999].

[d] Based on *Bellon et al.* [1983].

Table 2. Trace Element, Hf (±2σ) Nd, and Pb Isotopic Compositions of CLIP Rocks[a]

Sample	Age (Ma)	Lu	Hf	$^{176}Hf/^{177}Hf_m$	$^{176}Lu/^{177}Hf$	$^{176}Hf/^{177}Hf_{in.}$	$^{176}Hf/^{177}Hf_t$	εHf_t	εNd_t	$^{206}Pb/^{204}Pb_t$	$^{207}Pb/^{204}Pb_t$	$^{208}Pb/^{204}Pb_t$	$\Delta \varepsilon Hf_t$	$\Delta^{207/204}Pb_t$
DSDP Leg 15														
146-1	90	0.31	1.60	0.283119 (11)	0.0282	0.283070	0.283080	10.9	7.7	19.046	15.594	38.747	−2.6	3.8
150-1	90	0.26	1.92	0.283104 (10)	0.0194	0.283070	0.283080	10.9	6.8	18.989	15.596	38.748	−1.4	4.7
151-1	90	0.32	4.77	0.283039 (8)	0.0098	0.283022	0.283031	9.2	4.8	19.422	15.592	39.224	−0.3	−0.4
151-2	90	0.32	4.69	0.283003 (8)	0.0097	0.282986	0.282996	7.9	4.9	19.356	15.586	39.134	−1.8	−0.3
152-1	75	0.45	2.41	0.283193 (11)	0.0267	0.283154	0.283162	13.8	9.4	19.092	15.602	38.629	−2.2	4.1
153-1	90	0.47	2.20	0.283111 (5)	0.0305	0.283058	0.283067	10.4	6.9	18.977	15.591	38.716	−2.1	4.3
Nicoya														
AN2	90	0.54	2.22	0.283104 (10)	0.0348	0.283043	0.283053	9.9	6.9	19.012	15.580	38.803	−2.5	2.8
AN14	90	2.28	1.36	0.283351 (9)	0.2409	0.282932	0.282942	6.0	7.0	19.153	15.555	38.831	−6.6	−1.3
BN31	90	0.15	0.44	0.283116 (11)	0.0483	0.283032	0.283041	9.5	7.0	19.024	15.570	38.740	−3.1	1.7
AN18	90	0.23	0.93	0.283126 (9)	0.0359	0.283063	0.283073	10.6	6.8	19.101	15.570	38.844	−1.7	0.8
AN46	90	0.56	3.36	0.283127 (9)	0.0239	0.283085	0.283095	11.4	6.9	19.003	15.545	38.723	−1.1	−0.5
AN72	90	0.30	1.39	0.283117 (9)	0.0308	0.283064	0.283073	10.6	6.5	19.165	15.568	38.969	−1.2	0.0
AN81	90	0.30	1.23	0.283128 (8)	0.0347	0.283067	0.283077	10.8	6.8	19.120	15.557	38.907	−1.5	−0.7
AN86	90	0.73	3.95	0.283136 (8)	0.0266	0.283090	0.283100	11.6	6.8	19.247	15.565	38.888	−0.7	−1.2
AN99	90	0.30	1.41	0.283119 (11)	0.0308	0.283065	0.283075	10.7	6.7	19.143	15.581	38.983	−1.5	1.5
AN110	90	0.31	1.39	0.283117 (7)	0.0317	0.283062	0.283072	10.6	6.9	19.187	15.560	38.877	−1.9	−1.1
BN17	90	0.44	2.33	0.283153 (11)	0.0268	0.283106	0.283116	12.2	7.0	19.067	15.552	38.729	−0.5	−0.6
BN19	90	0.26	1.15	0.283125 (11)	0.0322	0.283069	0.283079	10.8	6.9	19.238	15.568	38.963	−1.6	−0.9
Herradura														
AH5	85	0.39	1.68	0.283115 (8)	0.0333	0.283057	0.283069	10.5	6.6	19.044	15.570	38.839	−1.5	1.5
AH8	85	0.26	1.13	0.283121 (11)	0.0324	0.283064	0.283077	10.8	8.0	19.125	15.555	38.822	−3.2	−0.9
BH11	85	0.26	1.20	0.283118 (9)	0.0311	0.283064	0.283076	10.7	6.7	19.220	15.588	38.978	−1.5	1.3
Golfito														
GO1	80	0.68	3.09	0.283151 (11)	0.0317	0.283102	0.283110	12.0	7.6	18.822	15.552	38.522	−1.4	2.0
GO2	80	0.42	1.85	0.283169 (10)	0.0327	0.283119	0.283127	12.6	7.1	19.018	15.564	38.651	−0.2	1.1
GO4	80	0.33	1.79	0.283107 (7)	0.0262	0.283066	0.283075	10.7	7.9	18.950	15.555	38.640	−3.1	1.0
Burica														
BUR4	65	0.28	1.27	0.283133 (7)	0.0315	0.283094	0.283101	11.6	7.0	19.156	15.558	38.823	−1.0	−1.0
BUR11	65	0.33	1.73[b]	0.283105 (7)	0.0273	0.283070	0.283077	10.8	7.2	19.153	15.567	38.801	−2.1	0.0
BUR12	65	0.33	1.73[b]	0.283121 (7)	0.0273	0.283086	0.283093	11.4	7.3	19.159	15.575	38.807	−1.6	0.3
BUR13	65	0.39	2.19[b]	0.283101 (6)	0.0253	0.283069	0.283076	10.8	7.3	19.138	15.559	38.753	−2.2	−0.7
BUR14	65	0.33	1.73[b]	0.283136 (9)	0.0273	0.283102	0.283109	11.9	7.3	19.096	15.560	38.732	−1.2	−0.1
Quepos														
AQ22	60	0.29	3.98	0.283024 (6)	0.0103	0.283012	0.283019	8.7	5.8	19.318	15.590	39.039	−2.2	0.4
AQ8	60	0.33	4.10	0.283012 (7)	0.0116	0.282999	0.283005	8.2	6.1	19.235	15.582	38.947	−3.1	0.6
AQ16	60	0.27	3.20	0.282995 (9)	0.0120	0.282981	0.282988	7.6	5.9	19.360	15.593	39.077	−3.5	0.3

Table 2. (continued)

Sample	Age (Ma)	Lu	Hf	^{176}Hf/^{177}Hf$_m$.	^{176}Lu/^{177}Hf	^{176}Hf/^{177}Hf$_{in.}$	^{176}Hf/^{177}Hf$_t$	ε Hf$_t$	εNd$_t$	^{206}Pb/^{204}Pb$_t$	^{207}Pb/^{204}Pb$_t$	^{208}Pb/^{204}Pb$_t$	Δ εHf$_t$	Δ ^{207}/^{204}Pb$_t$
AQ19	60	0.34	4.24	0.283002 (5)	0.0117	0.282988	0.282995	7.9	5.8	19.263	15.584	38.942	−3.1	0.5
AQ28	60	0.14	1.77	0.283030 (7)	0.0114	0.283017	0.283023	8.9	5.7	19.210	15.566	38.895	−1.9	−0.7
AQ43	60	0.33	3.72	0.283054 (6)	0.0127	0.283039	0.283045	9.7	6.3	19.251	15.588	38.948	−2.0	1.0
Osa														
OS2	60	0.39	2.05	0.283094 (8)	0.0275	0.283062	0.283068	10.5	7.2	19.134	15.566	38.739	−2.5	0.1
OS6	60	0.41	1.46	0.283284 (7)	0.0398	0.283238	0.283244	16.7	9.9	18.620	15.516	38.188	0.0	0.7
OS9	60	0.25	1.22	0.283118 (7)	0.0298	0.283083	0.283090	11.2	6.9	18.754	15.587	38.585	−1.3	6.3
OS16	60	0.35	1.43	0.283251 (9)	0.0352	0.283210	0.283216	15.7	9.3	18.652	15.537	38.267	−0.2	2.4
Curacao														
CUR8	90	0.13	0.68	0.283115 (15)	0.0275	0.283067	0.283077	10.8	5.6	19.007	15.616	38.548	0.1	6.5
CUR14	90	0.16	0.79	0.283129 (8)	0.0283	0.283080	0.283089	11.2	5.6	19.212	15.585	38.891	0.5	1.1
CUR20	90	0.21	1.06	0.283140 (19)	0.0286	0.283090	0.283100	11.6	5.9	19.095	15.554	38.903	0.6	−0.7
CUR36	90	0.33	1.56	0.283103 (10)	0.0305	0.283050	0.283059	10.1	6.8	19.043	15.550	38.819	−2.2	−0.5
Columbia Western Cordillera														
VIJ1	90	0.61	3.13	0.283101 (7)	0.0278	0.283052	0.283062	10.2	6.6	19.327	15.580	39.091	−1.8	−0.6
BAR5	90	0.22	0.96	0.283119 (10)	0.0326	0.283063	0.283072	10.6	6.5	19.273	15.560	39.052	−1.3	−2.1
BAR7	90	0.22	1.18	0.283111 (10)	0.0269	0.283065	0.283074	10.7	5.5	19.311	15.602	39.224	0.2	1.7
CBU4	90	0.27	1.18	0.283136 (6)	0.0324	0.283079	0.283089	11.2	7.0	19.390	15.581	39.134	−1.5	−1.2
CBU12	90	0.58	2.93	0.283096 (8)	0.0283	0.283047	0.283057	10.1	7.6	19.192	15.565	38.892	−3.4	−0.7
CBU14	90	0.35	1.52	0.283092 (10)	0.0326	0.283035	0.283045	9.6	7.0	19.004	15.543	38.672	−3.0	−0.8
PAN6	90	0.34	1.58	0.283100 (10)	0.0312	0.283045	0.283055	10.0	6.4	19.225	15.569	38.951	−1.7	−0.6
Colombia: Serrania de Baudó														
SDB5	75	0.30	1.43	0.283114 (8)	0.0299	0.283071	0.283079	10.8	7.2	19.160	15.562	38.848	−2.1	−0.6
SDB8	75	0.33	1.99	0.283108 (8)	0.0238	0.283073	0.283081	10.9	7.5	19.154	15.553	38.804	−2.4	−1.4
SDB11	75	0.29	1.34	0.283112 (8)	0.0312	0.283067	0.283075	10.7	7.4	19.199	15.557	38.922	−2.5	−1.6
SDB13	75	0.18	0.88	0.283137 (13)	0.0297	0.283094	0.283102	11.7	7.5	19.086	15.553	38.721	−1.7	−0.7
SDB16	75	0.31	1.69	0.283109 (11)	0.0265	0.283070	0.283078	10.8	7.6	19.103	15.546	38.710	−2.6	−1.6
SDB18	75	0.38	1.58	0.283135 (8)	0.0345	0.283085	0.283093	11.3	7.3	19.105	15.548	38.767	−1.7	−1.4
SDB20	75	0.36	1.65	0.283131 (11)	0.0312	0.283086	0.283094	11.4	7.0	19.095	15.553	38.739	−1.3	−0.8
SDB21	75	0.29	1.34	0.283121 (10)	0.0304	0.283077	0.283085	11.1	6.7	19.275	15.565	38.900	−1.2	−1.6

[a] Age, Nd, Pb and trace element data are from *Hauff et al.* [2000a, 2000b]. Burica ages are based on *Hoernle et al.* [2002a]. εHf and εNd calculated relative to the chondritic values of 0.282772 and 0.512638, respectively. Values projected for today's isotope composition of the mantle source (t) using their initial composition and age from *Hauff et al.* [2000a, 2000b] and the parent/daughter ratios for OIB's from *Sun and McDonough* [1989]. See *Hauff et al.* [2000a, 2000b] for sample locations.
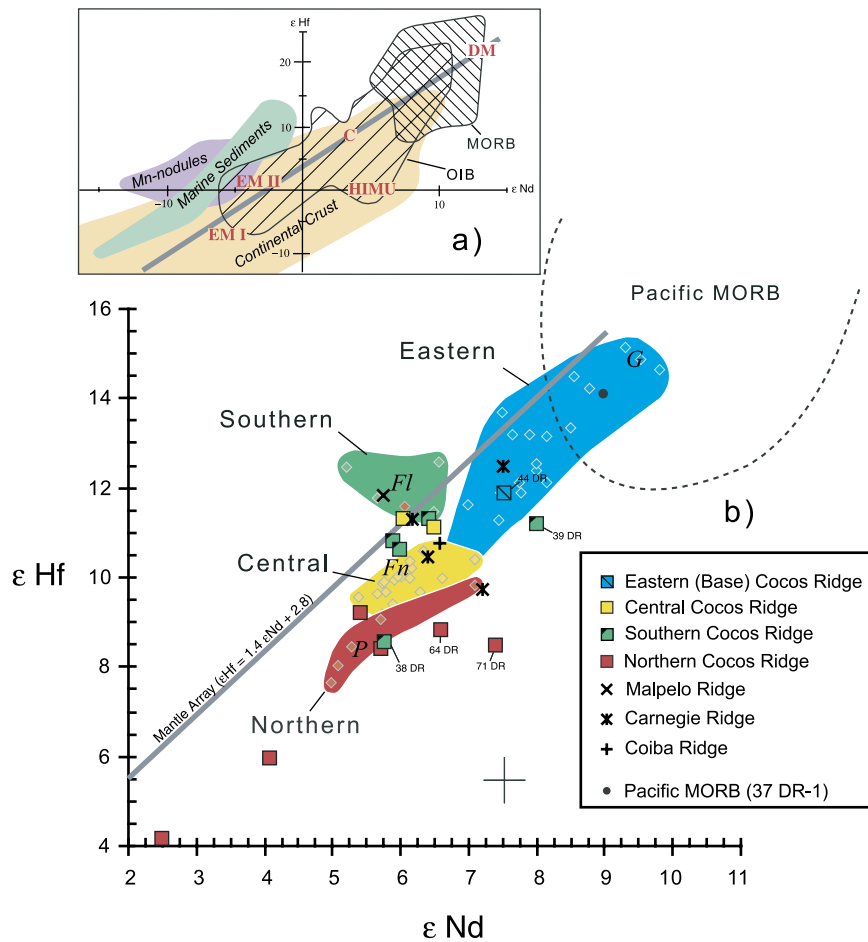[b] Hf concentrations not available and therefore the median of BUR 4 and BUR 13 is used.

Figure 4. (a) Global Nd versus Hf isotope mantle array (data from literature and unpublished data of J. Blichert-Toft); (b) εNd versus εHf ratios for submarine lavas of Cocos, Malpelo, Carnegie and Coiba ridges (Galápagos paleo-hot spot tracks). Cocos Ridge lavas are assigned to four sub-populations representing different geographic portions of the ridge (see text for details). The Nd data are from *Hoernle et al.* [2000] and Werner et al.(submitted manuscript, 2003). Indices (*Fl*, *Fn*, *P*, *G*) denote the average composition of the present-day Galápagos islands Floreana, Fernandina, Pinta and Genovesa. Also shown are the fields for the corresponding Galápagos domains as defined in Figure 2 based on data from *Blichert-Toft and White* [2001] (diamonds). The range and trends of the domains relative to the end-members islands (*Fl*, *Fn*, *P*, *G*) represent mixing (see text for explanation). One sample from northern Darwin Island (DA-1), located in the northern domain on Figure 2, plots as an outlier with εHf = +11.6 (small red diamond).

$^{206}Pb/^{204}Pb$, $^{207}Pb/^{204}Pb$ and $^{208}Pb/^{204}Pb$ but have low and high εHf, respectively. Two southern Cocos Ridge samples, 38DR-12 and 39DR-2 are more typical in terms of both εNd and εHf, of the northern and eastern Galápagos domains.

[13] Two northern Cocos Ridge lavas from Cocos Island and a nearby seamount (64DR-1 and 71DR-1, see sites on Figure 3) extend to slightly higher εNd values compared to the Galápagos northern domain field (Figure 4b). Lavas from

Cocos Island have been dated at 2 Ma [*Bellon et al.*, 1983] and therefore may not belong to the Cocos Ridge and Galápagos hot spot track but rather may represent a separate "Cocos Island magmatic event". Combined Sr, Nd and Pb isotope ratios, and now Hf isotopes as well, indicate that Cocos Island and Galápagos Island lavas have the same characteristic isotope signature [*Castillo et al.*, 1988; Werner et al., submitted manuscript, 2003; this paper]. The anomalously young volcanism of Cocos Island apparently represents plume material, perhaps under-plating the lithosphere, that became
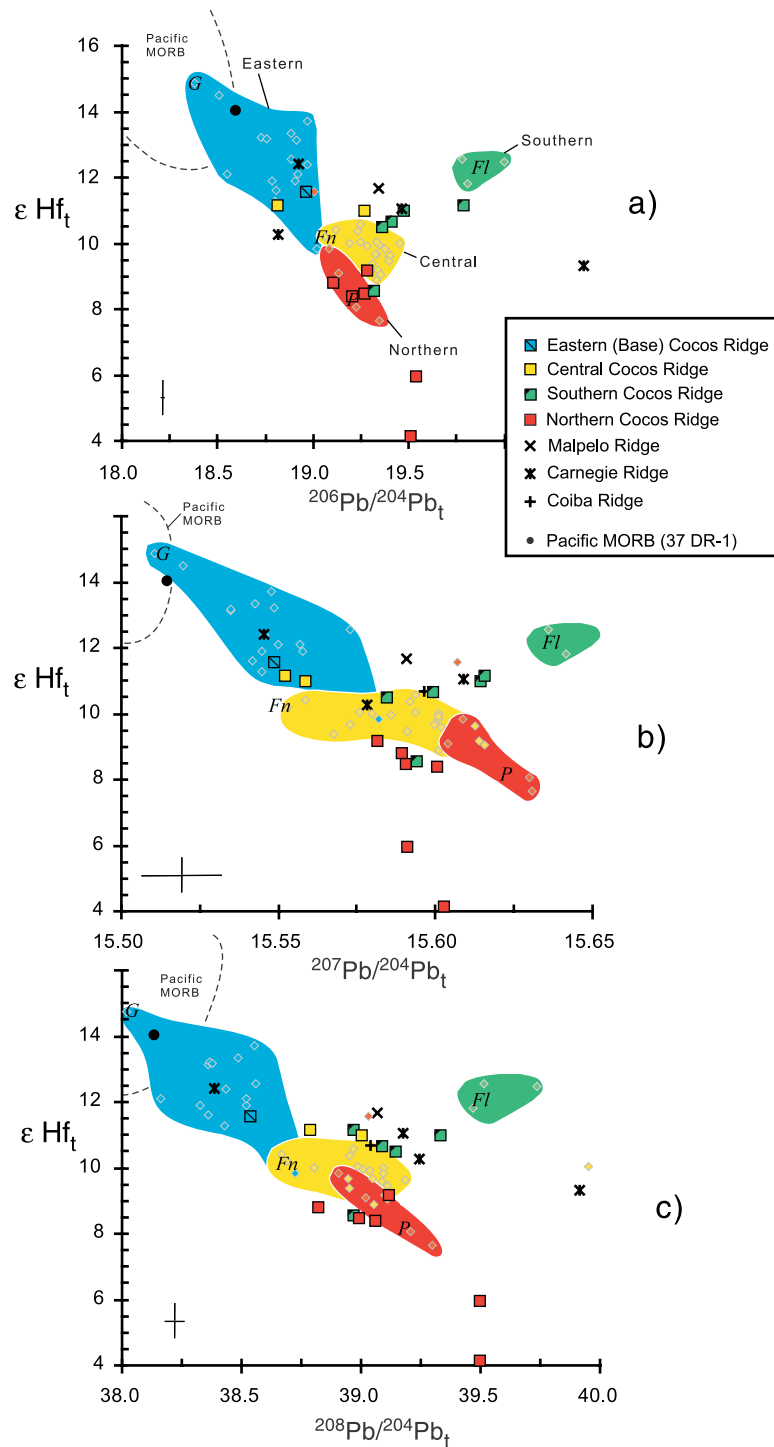
Figure 5. The topology of the Cocos ridge geographic domain sub-populations in Pb versus Hf isotope space is similar to the pattern of domains observed in the present-day Galápagos Archipelago (data sources given in Figure 4). The Pb data are from *Hoernle et al.* [2000] and Werner et al. (submitted manuscript, 2003). Indices *Fl*, *Fn*, *P*, *G* represent the isotopic composition of the Galápagos islands Floreana, Fernandina, Pinta and Genovesa. The Hf_t and Pb_t isotope data of Cocos Ridge suggest that the compositional fields of the northern Galápagos domain show a wider range than found in the present-day-Galápagos. This can be explained by compositional variation of the domains with time, different end-member mixing proportions, or perhaps this difference can be due to the limited number of available Hf isotope data from the northern Galápagos Islands.

reactivated at about 2 Ma by the initiation of a small and short-lived E-W striking intra Cocos Island spreading center [*Castillo et al.*, 1988, *Meschede et al.*, 1998, Werner et al., submitted manuscript, 2003]. The nearby seamount (site no. 71) is assumed to have formed at ∼5 Ma (see Table 1), which is in accordance with its position along the plume track.

[14] Cocos Ridge sample 44 DR-14, which has relatively low $^{206}Pb/^{204}Pb$, but more radiogenic Hf isotopes than other Cocos Ridge samples, plots in all figures within the field of the Galápagos eastern domain. It was dredged at the southern base of the Cocos Ridge. At 14 Ma the Galápagos spreading center was located above or to the south of the plume [*Werner et al.*, 1999]. If depleted melts formed by plume-ridge interaction in the southwest they were probably buried by enriched lavas as the plate moved to the northeast over the source regions of the northern, central and southern domains [*Hoernle et al.*, 2000]. Therefore sample 44 DR-14, which outcrops in a steep submarine valley near the base of the ridge, could represent the eastern domain lava type. This view is supported by the high εHf (Figure 4b) of this sample as well as its high εNd and relatively unradiogenic Pb isotopic composition (Figures 5a, 5b, and 5c) (Werner et al., submitted manuscript, 2003).

[15] The overall isotopic compositions of all analyzed rocks from the Malpelo, Coiba and Carnegie Ridges, including the Hf isotope data presented in this study, clearly overlap the present-day Galápagos and Cocos Ridge compositional fields (Figure 4b), thus supporting the model that these ridges are remnants of the Galápagos hot spot track [e.g., *Wilson and Hey*, 1995; *Hauff et al.*, 2000a; Werner et al., submitted manuscript, 2003]. The recognition of an analogously ordered geographic distribution of isotopic signatures in the Malpelo, Carnegie and Coiba Ridges similar to Cocos Ridge and present-day Galápagos is not observed in the few samples we have analyzed. This is not unexpected, because plate motion is at a high angle to the NE-SW orientation of the proposed geochemically striped zonation in the Galápagos plume [*Hoernle et al.*, 2000]. In contrast, the Cocos plate motion is sub-parallel to the orientation of the geochemical domains in the Galápagos archipelago, thus preserv-

ing the stripped geographic heterogeneity along the Cocos Ridge. The only sample from the Malpelo Ridge that could be attributed to the Floreana-like southern Galápagos domain, based on its elevated εHf with respect to its εNd (Figure 4b) and enriched $^{207}Pb/^{204}Pb$ (Figure 5), is 7 DR-1. Sample 17 TVG-1 from the southern Carnegie Ridge has relatively radiogenic Pb isotope ratios (e.g., $^{206}Pb/^{204}Pb$ and $^{207}Pb/^{204}Pb$ = 20.36 and 15.70 respectively), similar to the Floreana-like end-member, but has relatively low εHf, like the northern domain and Pinta Island. Three volcanic rocks dredged from the northern part of the Carnegie Ridge and the single sample from the western slope of Coiba Ridge have affinities with the central or northern domain compositions (Figure 4b).

3.2. Caribbean Large Igneous Province (CLIP)

[16] The isotope ratios of the CLIP volcanic rocks projected to the present-day (e.g., $εHf_t$, $^{206}Pb/^{204}Pb_t$ in the figures) show broad overlap and fall for the most part within the compositional fields for the central and eastern Galápagos domain fields (Figures 6 and 7). The CLIP lavas from Nicoya have Pb isotopes central to the present-day Galápagos domains, overlapping the central, northern and eastern fields, but range to higher $εHf_t$ (6.0–12.16). Burica, Golfito, and Herradura lavas exhibit strong affinities with the central domain field in Nd, Hf and Pb isotope diagrams (Figures 6 and 7). Quepos volcanics have Nd, Hf and $^{206}Pb/^{204}Pb_t$ isotope ratios similar to Pinta and the northern domain, but $^{207}Pb/^{204}Pb_t$ and $^{208}Pb/^{204}Pb_t$ more like the central Galápagos domain. The Osa samples are notably depleted in terms of Nd, Hf and Pb isotope compositions, comparable to the Genovesa-like end-member and eastern domain. Two of the Osa lavas are the most depleted of all the Galápagos plume-related volcanics of this study in terms of $εNd_t$ (+9.4 to +9.9) and $εHf_t$ (+15.7 to +16.7). Although the Curaçao lavas have Pb isotope characteristics similar to the central domain, their relatively high $εHf_t$ for a given $εNd_t$ is a characteristic they share with the Floreana-like end-member and the southern domain. The Columbian CLIP lavas are
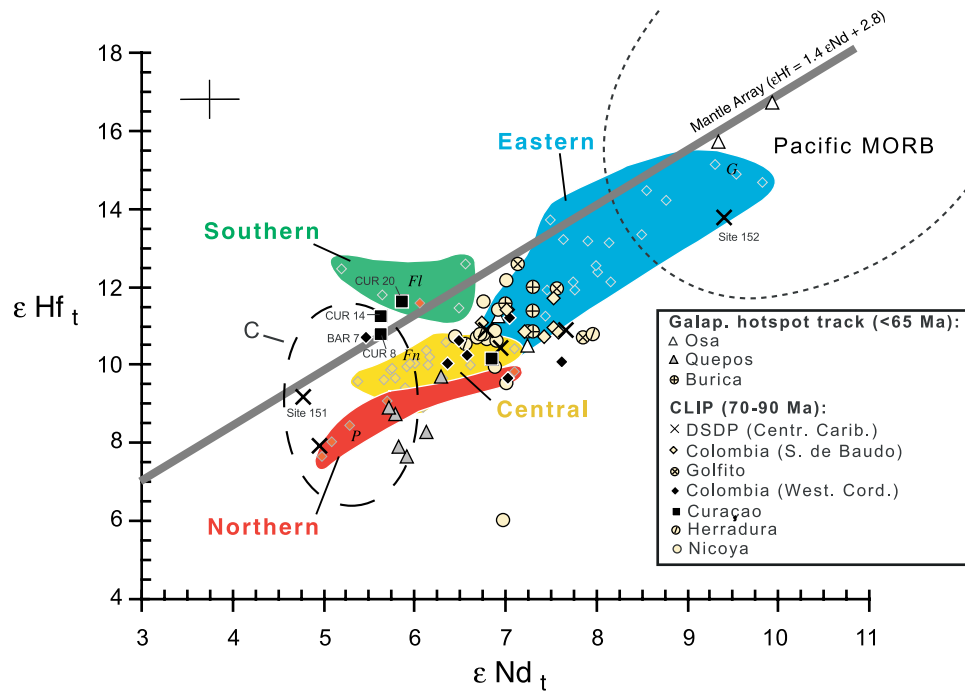
Figure 6. Quepos and Osa lavas have εNd_t and εHf_t signatures (projected to "zero age" as described in the text) that plot in the central/northern and eastern Galápagos domains, respectively. Lavas from Curaçao and the western Cordillera define elongate fields within the central Galápagos domain that trend toward the southern Galápagos domain. The line corresponds to the Global OIB εNd versus εHf regression line of Blichert-Toft (personal communication; see text). The striped field represents the composition of the mantle component C [*Hanan and Graham*, 1996; *Hanan et al.*, 2000]. The Nd data is from *Hauff et al.* [2000a, 2000b].

analogous to the central domain in terms of Pb isotopes, but one Western Colombia sample (BAR 7) has high southern domain-like εHf_t relative to its εNd_t. There are no CLIP lavas with the complete Floreana-like southern domain signature in all three isotope systems, Pb, Hf and Nd, which may reflect a greater sensitivity to alteration of the Pb isotope system than of the Nd [*Hauff et al.*, 2000b] and Hf isotope systems. Therefore the Nd and Hf isotope data should provide a more reliable estimate of the source components in the CLIP magma. However, the Curaçao samples with southern domain-like εHf-εNd have Pb isotope compositions that plot on the NHRL, which is not expected for samples undergoing submarine alteration and interaction with seawater and sediment.

[17] The CLIP lavas that consistently plot in the eastern Galápagos domain field in different Pb, Nd, Hf multiisotope binary projections are rare, except for Osa and several of the Golfito lavas. Pinta-like isotopic compositions that overlap the northern domain field are not observed in the CLIP except

for the Quepos samples. However, the Quepos and Osa (as well as Burica) magmatic complexes (54–65 Ma) are interpreted to represent post-CLIP ocean island volcanism along the early Galápagos hot spot track [*Hauff et al.*, 1997, 2000a; *Hoernle et al.*, 2002a]. We will return to these observations in the ensuing discussion.

4. Discussion

4.1. Galápagos Domains

[18] When the average position of the representative isotopic end-members Pinta, Fernandina, Floreana and Genovesa are considered along with the shape and trend of the corresponding fields for the proposed northern, central, southern and eastern domains (as defined by *Hoernle et al.* [2000]), it is apparent that mixing between end-members has taken place. The fields are interpreted by *Blichert-Toft and White* [2001] as three trends, corresponding to the Northern field (Wolf, Darwin, Pinta, Marchena), the Southern field (Floreana, San
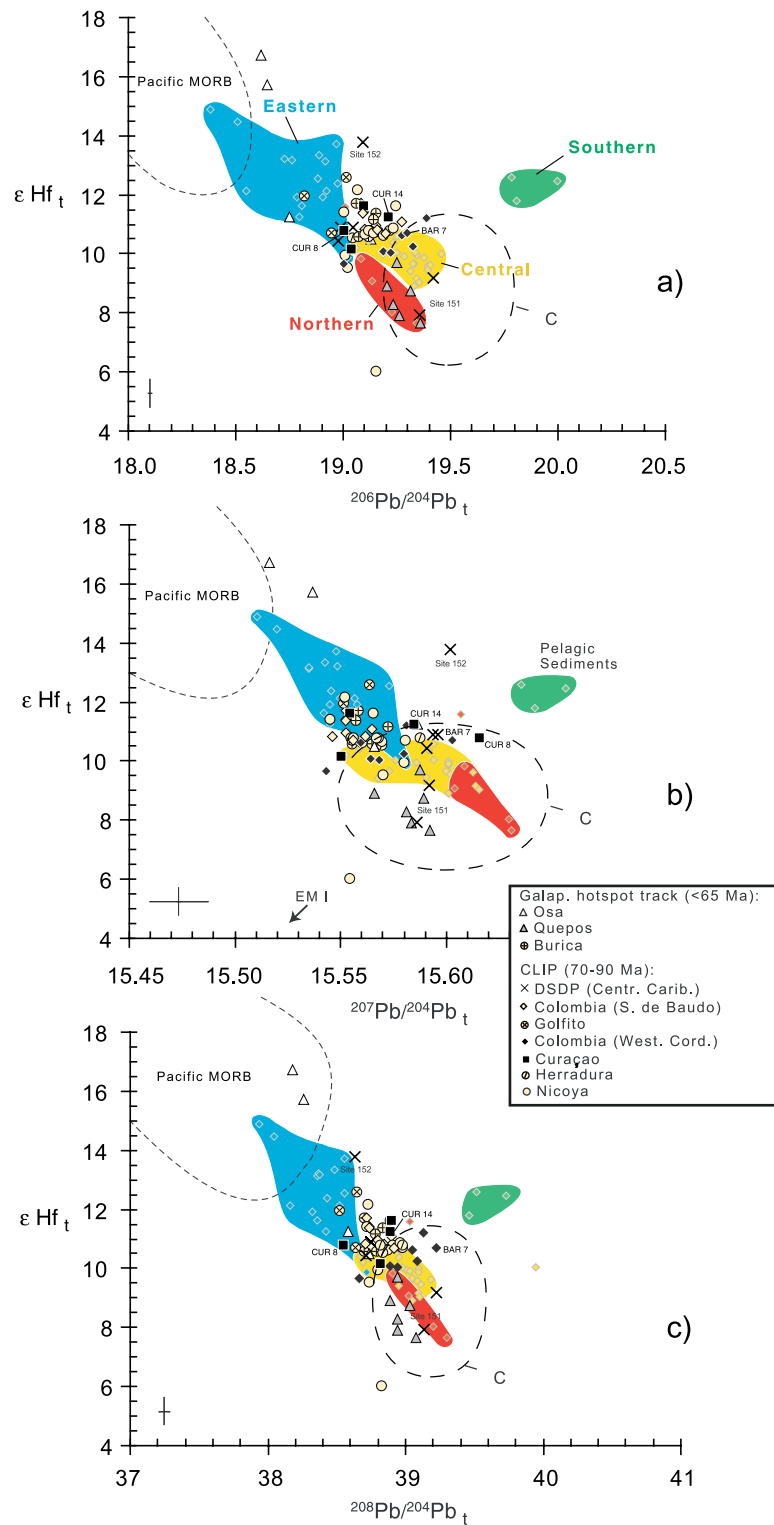
Figure 7. The CLIP lavas have Pb$_t$ and εHf$_t$ isotope signatures that for the most part are like the central domain (and eastern). Quepos and Osa have central/northern and eastern-like domain compositions, respectively.

Cristobal, Espanola) and the Central field (Santa Cruz, Roca Redonda, Isabela, Fernandina). They (op. cit.) interpreted the depleted component as the regular upper-mantle asthenosphere MORB source. In this interpretation the three enriched end-members have mixed extensively with the depleted source, but not much with each other [*Blichert-Toft and White*, 2001]. This is also illustrated by the shape and much larger size of the eastern domain field (Figure 4 and all following figures). The data presented in the present paper allow for a ~90 m.y. temporal perspective on the Galápagos plume source from the combined Pb-Nd-Hf isotope point of view. With this new perspective we can now constrain the role of the different end-members over time and refine models for the Galápagos mantle source mixing dynamics as observed in the present-day Galápagos domains.

[19] The central domain Galápagos component, characterized by Fernandina Island with high ^{3}He/^{4}He, is considered to represent the primary composition of the Galápagos plume source [*Graham et al.*, 1993; *Kurz and Geist*, 1999; *Harpp and White*, 2001; *Blichert-Toft and White*, 2001]. In Sr, Nd, Hf and Pb isotope space, the central domain closely resembles the isotopic signature of C-FOZO-PHEM, the common component of plumes [e.g., *Hart et al.*, 1992; *Farley et al.*, 1992; *Hanan and Graham*, 1996]. In the εNd versus εHf diagram, the central domain plots below the mantle array regression line (εHf = 1.4 * εNd + 2.8; Blichert-Toft, personal communication) with negative ΔεHf (where ΔεHf = εHf − 1.4 * εNd + 2.8). The northern domain component has higher Δ^{207}Pb/^{204}Pb and Δ^{208}Pb/^{204}Pb (relatively greater ^{207}Pb/^{204}Pb and ^{208}Pb/^{204}Pb for a point with the same ^{206}Pb/^{204}Pb relative to the Northern Hemisphere Reference Line (NHRL) of *Hart* [1984]), (Figures 8 and 9a), and extends to lower εNd, εHf and higher ^{87}Sr/^{86}Sr compared to the central domain. The Pinta-like northern domain Hf isotope compositions, except for one sample, plot below the mantle array in the εNd versus εHf diagram and below the central domain trend (Figures 4 and 6). The northern domain has low ^{3}He/^{4}He (8.8−6.9 R/R$_A$) [*Graham et al.*, 1993; *Kurz and Geist*, 1999] relative to the central (13.7−27.4 R/R$_A$) and eastern (8.6−

12.4 R/R$_A$) domains. The comparatively lower ^{3}He/^{4}He in the northern domain may result from preferential degassing of less radiogenic He [*Kurz and Geist*, 1999] or alternatively reflect different source compositions [*Harpp and White*, 2001; *Blichert-Toft and White*, 2001].

[20] In ^{207}Pb/^{204}Pb versus ^{206}Pb/^{204}Pb space, the Galápagos central and northern domain lavas show a similar range in ^{206}Pb/^{204}Pb and define steep, near vertical trends toward higher ^{207}Pb/^{204}Pb ratios (Figure 8a). Trends to higher Δ^{207}Pb/^{204}Pb could be explained by a very small addition of modern ocean seafloor sediment (<1%) to a composition lying on the NHRL (Figure 8a). However, the curvature of a mixing hyperbola in a plot of εNd versus εHf (Figure 9b) suggests involvement of a pollutant having sedimentary Pb isotope characteristics but relatively low Pb/Hf and high Hf/Nd. Mixing of the central domain source material with bulk pelagic sediment (or an EM I-like OIB mantle source; Figure 4a) therefore does not readily explain the low ΔεHf of the northern domain, but mixing with a hydrothermally altered oceanic crust-lithosphere could possibly account for these observations.

[21] The southern Galápagos component is typified by lavas from Floreana that have high εHf for a given εNd and ^{87}Sr/^{86}Sr, but enriched radiogenic HIMU-like Pb isotopic compositions [*Harpp and White*, 2001; *Blichert-Toft and White*, 2001]. In εNd-εHf correlation diagrams (Figures 4b and 6) southern domain lavas are displaced to the left of the mantle array (positive ΔεHf). Several possible scenarios that would allow the generation of a source isotope signature above the εNd-εHf mantle array are: (1) ancient melt extraction [e.g., *Salters and Hart*, 1991]; (2) carbonatite metasomatism; (3) recycling of subduction modified oceanic lithosphere; (4) shallow level contamination with modern pelagic sediment (e.g., assimilation of sediment, altered lithosphere or associated fluids); or (5) recycled pelagic sediment intrinsic to the magma mantle source [*Blichert-Toft et al.*, 1999]. We will now consider each of these possibilities.

[22] Ancient melt extraction at a depth where the garnet/clinopyroxene ratio was relatively high
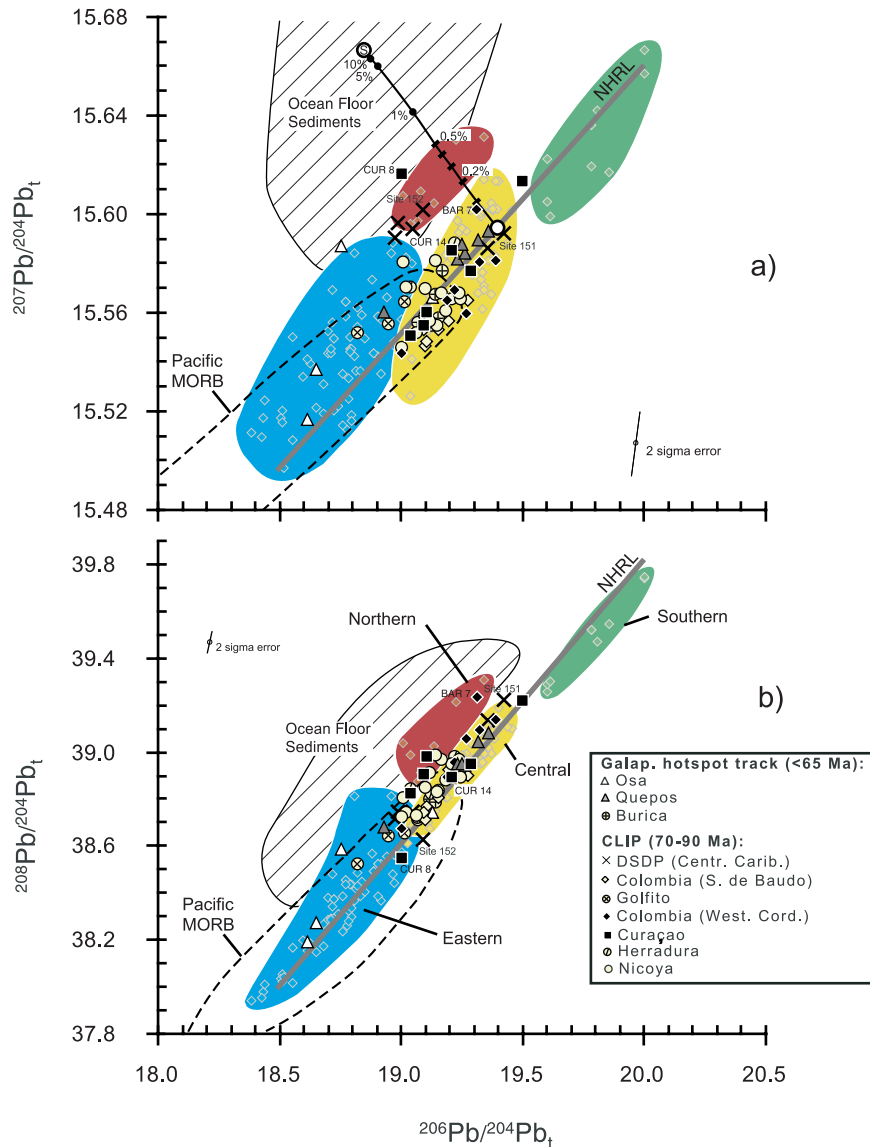
Figure 8. Curaçao and western Cordillera samples CUR 8 and BAR 7 have $^{206}Pb/^{204}Pb_t$, $^{207}Pb/^{204}Pb_t$ and $^{208}Pb/^{204}Pb_t$ isotope signatures that plot in the northern and central Galápagos domain fields, but their εHf_t and εNd_t are more similar to the Galápagos southern domain field (Figure 6). The Galápagos northern domain is characterized by relatively high $\Delta^{207}PB/^{204}Pb$ (i.e., it lies above the NHRL). The trend to high $\Delta^{207}Pb/^{204}Pb$, also seen in the central domain, but to a lesser extent, could be explained by a very small addition of modern seafloor sediment (S) < 0.1% (details in Figure 9). Galápagos Pb isotope data from *White et al.* [1993] and *Kurz and Geist* [1999], field for modern ocean floor sediment composition and average of $^{206}Pb/^{204}Pb = 18.84$, $^{207}Pb/^{204}Pb = 15.67$ used for simple bulk mixing calculation from *Ben Othman et al.* [1989].

could create a residue with an elevated (Lu/Hf)/(Sm/Nd) ratio [e.g., *Salters and Hart*, 1989, 1991; *Blichert-Toft and White*, 2001]. However, at greater depths U and Th should be even more incompatible than Pb making it difficult to explain the accompanying relatively radiogenic Pb isotopic signature without having to involve a modified recycled crustal component.

[23] In general, carbonatites are enriched in light rare earth elements, display positive anomalies for Sr and Ba, and are strongly depleted in Zr, and thus by inference, Hf [e.g., *Hoernle et al.*, 2002b; *Bell and Tilton*, 2001; *Ionov*, 1998]. Therefore carbonatitic melts, if solidified and stored in the mantle as veins or pockets, should develop high εHf while having essentially "normal" εNd. If assimilation of
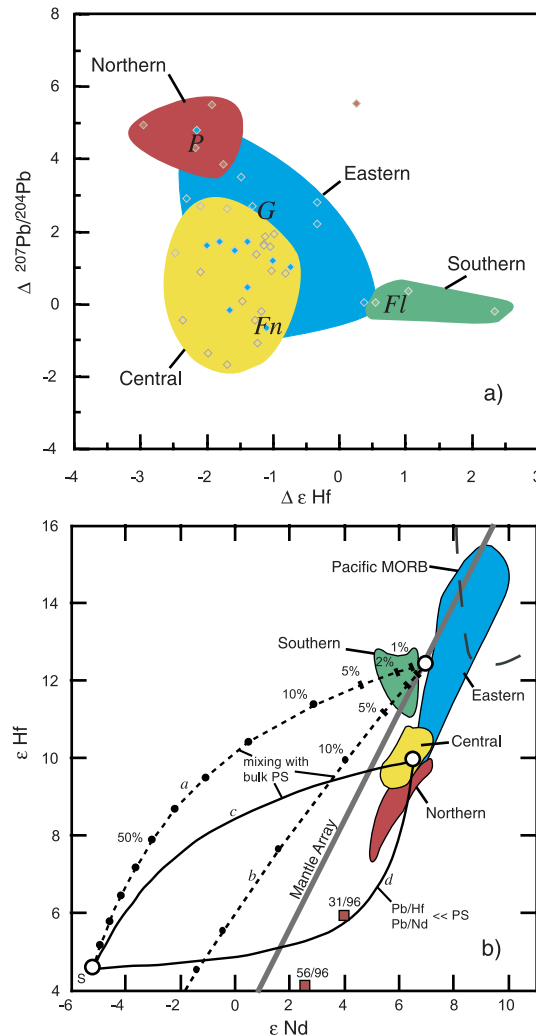
Figure 9. (a) The three enriched Galápagos domains, represented by the islands Pinta, Fernandina and Floreana (*P, Fn, Fl*) define distinct fields in ΔεHf and Δ^{207}PB/^{204}Pb isotopic space. The eastern domain which is similar to the Pacific MORB field overlaps the three enriched domains. (b) Binary mixing between the mantle array (eHf = 12.6, eNd = 7, Nd ppm = 13.15, Hf ppm = 2.94) and average ocean floor sediment (S) [e.g., *Ben Othman et al.*, 1989] requires bulk addition of at least ∼3% sediment (dashed curve a) to account for the positive ΔεHf in the southern Galápagos domain. The mixing curves were calculated using 4 ppm Hf, 60 ppm Nd, εNd = −5.3 for average Pacific sediments (S) [*Ben Othman et al.*, 1989] with an assumed εHf = −4.6. If marine sediment approach the trench its composition could be affected by increasing contribution of continental sediments with generally less radiogenic Hf and Nd isotope compositions resulting in a GLOSS-like composition (Global Subducting Sediment [*Planck and Langmuir*, 1998]). Using the GLOSS sediment composition, with εNd = −8.93, 4.1 ppm Hf, 27 ppm Nd and an asumed εHf = −6, there is no significant change in the general position and scale units of the mixing curve (dashed curve b). However, for the northern domain, the curvatures of mixing hyperbolae in plots of εNd versus εHf (solid curves) and Δ^{207}PB/^{204}Pb (not shown) suggest involvement of a pollutant having more EM I-like, ocean-floor sediment Pb isotope characteristics but with relatively low Pb/Hf and Pb/Nd and high Hf/Nd. Pollution of the central domain (εNd = 6.5, εHf = 10.0, Nd ppm = 13.15, Hf ppm = 2.94) by bulk S does not readily explain the low εHf of the northern domain (curve c), but mixing with a component with hydrothermally altered trace element concentrations (45 ppm Hf, 15 ppm Nd) and isotopic composition resembling modern seafloor sediments may account for the observations (curve d). The combined Hf-Nd isotopic data of Quepos and northern Cocos Ridge extend the Galápagos northern domain to far lower εHf and εNd than shown here (based on only 8 available Hf/Nd data from the Wolf-Darwin region). Note that the Cocos Ridge samples 31/96 and 56/96 fall close to the proposed northern domain mixing hyperbolae.

carbonatitic veins is responsible for the positive $\Delta\varepsilon$Hf signature of Floreana and the southern domain magmas, then we should also see evidence in the trace element signature of these lavas. On the basis of the available trace element data [*Kurz and Geist*, 1999; *White et al.*, 1993], Floreana lavas have relatively elevated Ba and Sr concentration levels and high concentrations of Rb, Th, U, Pb, and La as well as additional features that point in the direction of possible regional mantle metasomatism as also noted by *Harpp and White* [2001]. However, these trace element variations would also be consistent with the presence of ocean floor sediment or recycled pelagic sediments in the mantle source. Trace element ratios that are independent from sediment contribution but more specific to carbonate metasomatism, such as Yb/Zr, on the other hand, are not significantly higher in Floreana lavas compared to other Galápagos islands. In addition, there is no apparent correlation between Yb/Zr and Ba/Zr or $\Delta\varepsilon$Hf in Floreana lavas. Our observations are, however, based on only few available Zr concentration data from the literature and these data, unfortunately, are rarely from the same samples from which Hf isotopes where also measured. Further combined trace element and isotope studies of Floreana and other Galápagos end-member lava samples are therefore required to unambiguously address this question.

[24] An alternative scenario is that the higher (Lu/Hf)/(Sm/Nd) ratios of the southern domain source occur during subduction of hydrothermally altered oceanic crust. The lower gabbroic crust is converted to eclogite during subduction, which has a higher garnet-to-clinopyroxene ratio than basaltic ocean crust. In this case, the southern component could represent hydrothermally altered gabbroic portions of recycled oceanic crust. On the basis of the present Hf isotope data it is not possible to rule out this interpretation, but trace element signatures of lavas from the Floreana region indicate an absence of garnet in the southern Galápagos domain source [*Harpp and White*, 2001].

[25] Compared to the other Galápagos lavas, southern domain lavas are displaced toward marine sediments in εNd-εHf space (Figure 4a). Pelagic sediment can develop positive $\Delta\varepsilon$Hf because ele-

mental Hf trapped in the heavy refractory mineral zircon remains in shelf sediments [*Patchett et al.*, 1984]. Some Hawaiian basalts, interpreted to have a component of pelagic sediment in their mantle source, have similar high εHf and positive $\Delta\varepsilon$Hf, but an accompanying Pb isotope signature comparable to ancient recycled pelagic sediment with EM I-like low ^{206}Pb/^{204}Pb and positive Δ^{207}Pb/^{204}Pb and Δ^{208}Pb/^{204}Pb [*Blichert-Toft et al.*, 1999]. In contrast, the Floreana lavas have high ^{206}Pb/^{204}Pb more similar to modern pelagic sediment but ^{207}Pb/^{204}Pb and ^{208}Pb/^{204}Pb ratios that plot essentially on the NHRL. A Pb isotope signature on the NHRL argues against assimilation of pelagic sediment because the typical Pb isotope composition of pelagic sediment is characterized by $+\Delta^{207}$Pb/^{204}Pb and $+\Delta^{208}$Pb/^{204}Pb. A possible scenario could be that the Hf and Pb isotope compositions represent relatively young recycled and chemically modified subducted oceanic lithosphere containing a marine sediment component [e.g., *Hanan and Graham*, 1996; *Blichert-Toft et al.*, 1999]. Binary mixing between a composition on the mantle array and marine sediment [e.g., *Ben Othman et al.*, 1989; *Planck and Langmuir*, 1998] would require bulk addition of ~3% sediment to account for the $+\Delta\varepsilon$Hf in the southern Galápagos domain (Figure 9b). The combination of $+\Delta\varepsilon$Hf and a Pb isotope signature falling on the NHRL could result from a scenario where the relatively high U and Pb concentrations and high U/Pb ratio in the incorporated sediment component dominate the Pb isotope composition of the modified lithosphere and cause relatively rapid in-growth of radiogenic ^{206}Pb by ^{238}U decay, with essentially no apparent changes in radiogenic ^{207}Pb or ^{208}Pb. This would happen because most of the ^{235}U (which decays to ^{207}Pb) decayed away early in Earth's history due to its relatively short half-life and because the half-life of ^{232}Th (which decays to ^{208}Pb) is an order of magnitude longer than ^{238}U (which decays to ^{206}Pb) thus resulting in far less in-growth of ^{208}Pb in the same time span that produces significant in-growth of ^{206}Pb. In other words, the radiogenic growth of ^{206}Pb dominates the magnitude and direction of the radioactive decay path on Pb-Pb isotope diagrams. This could result in the loss of the $+\Delta^{207}$Pb/^{204}Pb and $+\Delta^{208}$PB/^{204}Pb signatures characteristic of marine

sediment in time periods on the order of hundred(s) of million years.

[26] The Genovesa-like end-member component of the eastern domain represents the depleted material in Galápagos plume mixing models [*White et al.*, 1993; *Hoernle et al.*, 2000; *Hauff et al.*, 2000a; *Harpp and White*, 2001; *Blichert-Toft and White*, 2001]. *Harpp and White* [2001] and *Blichert-Toft and White* [2001] note that the Nd-Sr-Pb-Hf isotope and trace element compositions of the eastern Galápagos depleted component are identical to "zero-age" Pacific MORB, and therefore consider it to represent the ambient depleted upper mantle MORB source. They interpret principal component analysis of the Pb, Hf, Nd and Sr isotope ratios as showing three distinct mixing trends that result from mixing between the three incompatible element enriched and distinct isotopic Galápagos plume end-member components and the ambient depleted MORB source. The Galápagos southern, northern and central domains would represent geographic regions where mixing is dominated by the individual end-members interacting with the depleted mantle to produce the three separate arrays in εHf, $^{206}Pb/^{204}Pb$, $^{87}Sr/^{86}Sr$ and εNd multiisotope space [*Blichert-Toft and White*, 2001]. This interpretation requires that mixing between the three plume components is minor compared to mixing between the depleted end-member and each individual plume component and that the last source mixing event is between the individual plume components and the depleted source. Because the plume traverses the depleted upper mantle as it rises and melts they argue that it is likely the depleted source is the regular depleted upper mantle rather than an intrinsic plume component. However, it cannot be ruled out that MORB source material is entrained in the plume stem at greater depth (>100 km) or that the depleted component is recycled lower oceanic crust and that mixing between enriched and depleted material occurs within the plume.

4.2. CLIP Pb-Nd-Hf Isotope Signatures

[27] Low-temperature seawater alteration and hydrothermal interaction have variably affected the isotope systematics of the ancient CLIP lavas.

In particular, Rb and Sr show high degrees of mobility, some samples show redistribution of elemental U, Th and Pb, but the rare earth elements Sm and Nd seem to be only slightly affected [*Hauff et al.*, 2000b]. Because Lu and Hf are presumably even more refractory than Sm and Nd, the Hf isotopes are relatively insensitive to secondary processes. Hf isotopes thus add a different perspective to the isotope systematics and may allow the identification in greater detail of the starting plume-head isotopic composition and nature of the plume components.

4.3. Nicoya, Herradura, and Golfito

[28] The Nicoya, Herradura, and Golfito complexes and the Caribbean seafloor are interpreted to be derived from the initiation of the Galápagos plume at 95–70 Ma and represent the Caribbean LIP basement [e.g., *Sinton et al.*, 1998; *Hauff et al.*, 1997, 2000a, 2000b]. The Sm-Nd and U-Pb isotope and trace element data are consistent with a mantle source origin involving a recent recycled oceanic lithosphere (300–500 million years old) component [*Hauff et al.*, 2000b]. Relative to the present-day Galápagos domains, Nicoya and Herradura show mainly central domain-like Pb-Nd-Hf isotope characteristics. Golfito shows primarily central domain characteristics except for several samples that plot consistently in the eastern domain field in the Pb-Nd-Hf isotope space. In general, all of these terranes show some overlap with the eastern domain field in multiisotope space suggesting contribution from the depleted source component during the plume-head stage.

4.4. Curaçao, Western Colombia and CLIP DSDP Leg 15

[29] Most lavas from Curaçao and western Colombia have central Galápagos domain Pb-Nd-Hf isotope characteristics. However, several CLIP lavas from Curaçao (samples Cur 8, Cur 14, and Cur 20) and one from the Western Colombian Cordillera (BAR7) have relatively high $\Delta \varepsilon Hf$ and plot with the Galápagos southern domain data in the εNd_t versus εHf_t diagram (Figure 6). However, in $^{206}Pb/^{204}Pb_t$ versus $^{207}Pb/^{204}Pb_t$ and $^{208}Pb/^{204}Pb_t$ diagrams (Figure 8)

samples CUR 8 and BAR7 do not show southern domain isotope characteristics. Rather, they plot in the less radiogenic northern and central Galápagos domain fields (Figure 8a). In both diagrams (Figures 6 and 8a), these two samples could in part reflect dilution by the northern or central domain components. Problems with accurately determining primary Pb isotopic compositions of altered and aged submarine erupted lavas could also result in less radiogenic calculated Pb isotope initial ratios as discussed in detail by *Hauff et al.* [2000b]. Both lavas show evidence for Pb gain, but it is unlikely that this is a secondary post emplacement alteration effect because there is no evidence for redistribution of U relative to Th [*Hauff et al.*, 2000b]. Furthermore, the measured $^{206}Pb/^{204}Pb$ and $^{207}Pb/^{204}Pb$ ratios of samples Cur 8, Cur 14, Cur 20 and Bar 7 do not exceed 19.35 and 15.61 [*Hauff et al.*, 2000a, 2000b], respectively, and would still plot well below the southern domain field in Figure 8a. The combined high $\Delta\epsilon Hf_t$ and $\Delta^{207}Pb/^{204}Pb_t$ signature for samples CUR 8 and BAR7 relative to their $^{206}Pb/^{204}Pb_t$ is therefore more likely explained by contamination with a sediment component having a time-integrated Pb, Nd and Hf isotopic evolution similar to that of modern-day seafloor sediments. Although it would take only a very small amount of pelagic sediment, less than 0.5%, to account for the high $\Delta^{207}Pb/^{204}Pb$ in CUR 8 and BAR7 (Figure 8a) it would take significantly more sediment contamination, on the order of several percent, to account for the high $\Delta\epsilon Hf$ (Figure 9b). Ancient melt extraction at a depth where the garnet/clinopyroxene ratio was relatively high also cannot explain the elevated $\Delta\epsilon Hf$ of CUR 8 and Bar 7 because their Sm/Nd and Lu/Hf ratios are not consistent with reasonable mantle melting paths; the lavas have low initial $^{143}Nd/^{144}Nd$ ratios compared to their Sm/Nd ratio but $^{176}Hf/^{177}Hf$ ratios consistent with their Lu/Hf ratios [e.g., *Chauvel and Blichert-Toft*, 2001]. Therefore the most likely explanation for the unusual isotopic composition of these two samples is assimilation of hydrothermally altered ocean crust and/or associated pelagic sediment during eruption similar to the process already discussed for the origin of the northern domain

signature (and also discussed by *Kerr et al.* [1996] for some of the Curaçao basalts). The other Curaçao lavas with high positive $\Delta\epsilon Hf$ (Cur 14 and Cur 20) do not have unusually high $\Delta^{207}PB/^{204}Pb$, consistent with contribution from a recycled pelagic sediment component, such as that postulated for the southern Galápagos domain mantle source.

[30] The DSDP samples 146-1, 150-1, 152-1, and 153-1 likewise have high $\Delta^{207}PB/^{204}Pb$ but ϵNd_t and ϵHf_t ratios that fall within the mantle array, suggesting influence of a seafloor sediment component. As has been pointed out by *Hauff et al.* [2000b], however, the uppermost plateau lavas sampled during Leg 15 in the Caribbean Sea were severely affected by seawater alteration/metamorphism and for this reason the Pb isotopic compositions must be treated with caution. Therefore the Nd and Hf isotope data again provide us with the best insight into the source compositions of these lavas. DSDP Leg 15 samples from Sites 146-1, 150-1, 152-1, and 153-1 overlap the central and eastern domain fields of the Galápagos Archipelago on the ϵNd_t versus ϵHf_t diagram, whereas the Site 151 samples plot close to the northern domain field.

4.5. Quepos, Osa and Burica

[31] Quepos is thought to represent seamount/ocean island volcanism active between 59 and 65 Ma; Osa and Burica terranes appear to be accreted tholeiitic aseismic ridges (similar to the Cocos and Carnegie ridges) formed between 54 and 64 Ma [*Sinton et al.*, 1997; *Hauff et al.*, 2000a; *Hoernle et al.*, 2002a]. The Pb, Nd and Hf isotopes of these three terranes span nearly the entire range of variation shown by the CLIP. The Quepos lavas have Nd, Hf and Pb isotope signatures similar to the present-day central and northern Galápagos domains (Figures 6–8). The Osa tholeiites have depleted Pb, Hf, and Nd isotope signatures, extending to even more depleted compositions than the eastern Galápagos domain (Figure 6). Burica lavas have intermediate compositions, similar to the enriched end of the eastern domain. The new Hf isotope results are consistent with the interpretation that Quepos and Osa are part of the Galápagos hot

spot track representing an ocean island and aseimic ridge, respectively, formed over the Galápagos plume tail after the CLIP drifted to the east relative to the hot spot.

5. Summary and Conclusions

5.1. CLIP

[32] Hafnium isotopes for the CLIP lavas from Costa Rica, Curaçao, Western Colombia, and central Caribbean DSDP sites, in conjunction with published Pb and Nd isotopes show that the central Galápagos Fernandina-like component was the dominant composition of the early Galápagos plume head. The CLIP lavas studied here have $^{206}Pb/^{204}Pb_t$ ratios within the range exhibited by lavas from the present-day central Galápagos domain. In general, the individual CLIP terranes display relatively steep trends in $^{206}Pb/^{204}Pb$ versus $^{207}Pb/^{204}Pb$ and $^{208}Pb/^{204}Pb$ diagrams, similar to the central Galápagos domain today. Trends such as these are expected for lavas derived from recycled oceanic crustal protoliths that have incorporated variable amounts of continental Pb prior to subduction during the past 200–2000 million years [e.g., *Hanan and Graham*, 1996, Figure 3]. The combined Hf-Nd isotope data of some Curaçao lavas suggest that the southern component can possibly be traced back for at least 90 Ma into the CLIP plume head. However, the Pb isotopes, projected to present-day values, never exceed $^{206}Pb/^{204}Pb$ values of 19.5, which does not support strong influence of a southern Galápagos domain component with relatively radiogenic Pb isotopes during the early Galápagos plume head stage and CLIP formation. Slightly positive $\Delta\epsilon Hf$ suggests that two CLIP lavas, from Curaçao (CUR8) and western Columbia (BAR7), may have a sediment component with Pb and Hf isotope signatures more similar to modern seafloor sediments [e.g., *Cousens et al.*, 2002; *Vervoort et al.*, 1999] rather than recycled pelagic sediment as discussed above for the southern component (Figure 8). In contrast, the positive $\Delta\epsilon Hf$ of Curaçao samples CUR 20 and CUR 14 and Pb isotope ratios on the NHRL are consistent with a recycled pelagic sediment contribution as proposed for the origin of the characteristic isotope signature of the Floreana-like component and the southern Galápagos domain.

[33] There is no convincing evidence for negative $\Delta\epsilon Hf$ with Pb and Nd isotope characteristics of the northern Galápagos domain in the CLIP except possibly for two DSDP Leg 151 lavas. The Leg 151 lavas were erupted during the late stages of the CLIP formation suggesting that they may represent transition to the early plume tail stage. Most of the CLIP lavas, except for the few unusual samples with anomalously high positive $\Delta\epsilon Hf$, have Pb, Nd, and Hf isotope compositions resembling the depleted end of the central domain and forming near-linear trends in multiisotope space. In broad terms, these trends could result from binary mixing between a depleted eastern domain-like component and an enriched end-member similar to the enriched end of the central domain composition or the southern domain. Both the depleted and the enriched end-members may be intrinsic to the plume (e.g., part of a recycled oceanic crustal protolith) or alternatively the depleted component may represent the ambient upper mantle Pacific MORB source.

5.2. Early Hot Spot Track

[34] The Hf isotopes for the plume tail hot spot track Quepos, Osa, Burica, the Malpelo, Coiba, Cocos, and Carnegie ridge regions, clearly demonstrates that all three enriched Galápagos plume components and a depleted MORB-like component have contributed significantly to the Galápagos plume volcanism since about 65 Ma when the plume tail was no longer located beneath the thick CLIP plume head products.

5.3. Cocos Ridge

[35] The geographic distribution of the combined Nd, Sr and Pb isotope signatures along the Cocos Ridge is similar to the present-day Galápagos Archipelago. In detail the Hf isotopes of some samples exhibit inconsistencies between their geographic location and the predicted isotope signature. For example, as discussed above, there are samples of southern geographic origins, display-

ing northern (38DR-2) and eastern (39DR-2) εNd-εHf isotope characteristics (Figure 4). Furthermore, the distinction between the Cocos Ridge southern and central domains in εNd-εHf space (Figure 4) are not as clear-cut as they appear to be in Hf-Pb or Pb-Pb isotope diagrams (e.g., Figure 5 and *Hoernle et al.* [2000, Figure 2a]). Apparently, Pb isotope ratios are more sensitive in their ability to reveal plume pollutants than Nd and Hf isotopes [*Hanan et al.*, 1986]. Another related factor that could contribute to the discrepancies is rejuvenated magmatism along the Cocos Ridge, as discussed for sample 64 DR-1 from Cocos Island. Despite these potential complications, Hf along with Nd and Pb isotopes are consistent with the geographic location and Pinta-like isotope characteristics of a northern domain along the seamounts north of the Cocos Ridge and a central and/or southern domain paralleling it along the Cocos Ridge. The apparently more irregular and less common geographic and temporal occurrence of southern domain lavas relative to the Fernandina-like central domain plume end-member suggests that it may not necessarily be intrinsic to the plume, but might possibly represent a component picked up by the plume as it traverses through and is dispersed into the upper mantle.

5.4. Sediment Recycling

[36] As shown above, Hf isotopes suggest the possibility for two types of sediment components affecting the Pb-Nd-Hf isotope composition of the Galápagos hot spot lavas, a recycled pelagic sediment-like component ($\Delta^{207}PB/^{204}Pb \approx 0$, highly positive $\Delta\varepsilon Hf$) typical of the southern domain and a hydrothermal component with a more EM I-like Pb isotopic composition resembling modern seafloor sediments [e.g., *Ben Othman et al.*, 1989; *Cousens et al.*, 2002; *Vervoort et al.*, 1999] with high positive $\Delta^{207}PB/^{204}Pb$ and $\Delta^{208}PB/^{204}Pb$ and variable $\Delta\varepsilon Hf$ (e.g., the Pinta-like northern Galápagos domain, northern Cocos ridge, Quepos). The scarcity of Pinta-like northern domain compositions in the plume head-derived CLIP lavas and the presence of lavas with northern domain isotope characteristics in both the Galápagos Platform and

paleo-plume tail track could suggest that these isotope signatures may in part reflect upper mantle melting processes associated with plume- ridge or lithospheric interaction. The restriction of northern domain isotope compositions (high positive $\Delta^{207}PB/^{204}Pb$ and negative $\Delta\varepsilon Hf$) in the present-day Galápagos archipelago to the Wolf-Darwin lineament region (see Figure 2), where seismic experiments are interpreted to demonstrate that shallow mantle plume-ridge interaction is occurring [*Toomey et al.*, 2001] suggests that central domain-like plume material may be polluted as the plume flows beneath the lithosphere and is sheared and spread into the upper mantle toward the Galápagos spreading center [*Hauff et al.*, 2002]. Over the past 5 m.y. the ridge axis has migrated to the northeast relative to the hot spot [*Wilson and Hey*, 1995]. Numerous ridge-jumps and propagation events along the GSC have resulted in widespread faulting and shear deformation of the ocean crust, which may aid in opening cracks that become pathways for hydrothermal circulation, which would be more pervasive than in normal ocean crust [*Hey et al.*, 1980]. Such a mechanism may increase the possibility for shallow level pollution of the northward migrating plume material and account for the ocean floor sediment-like isotope signatures in the northern domain. Alternatively, the lithosphere may restrict melting to depths that favor greater influence of the northern component in melts derived from a heterogeneous plume as plume material migrates toward the GSC [e.g., *Geist et al.*, 1988; *White et al.*, 1993; *Hoernle et al.*, 2000; Harpp, K. S., W. Wanless, R. Otto, R. Werner, and K. Hoernle, The Cocos and Carnegie Ridges: A Record of Complex, Long-term Galápagos Plume-Ridge Interaction, manuscript in preparation, 2003] The apparent consistent geographic relationship between the northern and central domains may simply relate to the long-term close proximity of the GSC and the plume.

[37] A better understanding of the geochemical origin and evolution of the Galápagos Plume can perhaps only become more fully realized once the Pb, Nd, Hf and Sr isotope systematics can be combined with comprehensive trace element and

rare gas data on the same samples to reveal through statistical analyses and mathematical modeling [e.g., *White et al.*, 1993; *Hanan and Graham*, 1996, 2000] the geochemical processes responsible for the characteristic Galápagos end-member isotopic signatures.

Acknowledgments

References

Barckhausen, U., C. R. Ranero, R. von Huene, S. C. Cande, and H. A. Roeser, Revised tectonic boundaries in the Cocos plate off Costa Rica: Implications for the segmentation of the convergent margin and for plate tectonic models, *J. Geophys. Res.*, *106*, 19,207–19,220, 2001.

Bell, K., and G. R. Tilton, Nd, Pb, and Sr isotopic composition of East African carbonatites: Evidence for mantle mixing and plume inhomogeneity, *J. Petrol.*, *42*, 1927–1945, 2001.

Bellon, H., R. Saenz, and J. Tournon, K-Ar radiometric ages of lavas from Cocos Island (Eastern Pacific), *Mar. Geol.*, *54*, M17–M23, 1983.

Ben Othman, D., W. M. White, and J. Patchett, The geochemistry of marine sediments, island arc magma genesis, and crust-mantle recycling, *Earth Planet. Sci. Lett.*, *94*, 1–21, 1989.

Blichert-Toft, J., and W. M. White, Hf isotope geochemistry of the Galápagos islands, *Geochem. Geophys. Geosyst.*, *2*, Paper number 2000GC000138, 2001.

Blichert-Toft, J., C. Chauvel, and F. Albarède, Separation of Hf and Lu for high-precision isotope analysis of rock samples by magnetic sector-multiple collector ICP-MS, *Contrib. Mineral. Petrol.*, *127*, 248–260, 1997.

Blichert-Toft, J., F. Frey, and F. Albarede, Hf isotope evidence for pelagic sediments in the source of Hawaiian basalts, *Science*, *285*, 879–882, 1999.

Castillo, P., R. Batiza, D. Vanko, E. Malavassi, J. Barquero, and E. Fernandez, Anomalously young volcanoes on hotspot traces: I. Geology and petrology of Cocos Island, *Geol. Soc. Am. Bull.*, *100*, 1400–1414, 1988.

Chauvel, C., and J. Blichert-Toft, A hafnium isotope and trace element perspective on melting of the depleted mantle, *Earth Planet. Sci. Lett.*, *190*, 137–151, 2001.

Cousens, B. L., J. Blenkinsop, and J. M. Franklin, Lead isotope systematics of sulfide minerals in the Middle Valley hydrothermal system, northern Juan de Fuca Ridge, *Geochem. Geophys. Geosyst.*, *3*(5), 1029, doi:10.1029/2001GC000257, 2002.

Donnelly, T. W., K. Melson, R. Kay, and J. J. W. Rogers, Basalts and Dolerits of Late Cretaceous age from the Central Caribbean, *Initial Rep. Deep Sea Drill. Proj.*, *15*, 989–1012, 1973.

Duncan, R. A., and R. B. Hargraves, Caribbean region in the mantle reference frame, in *The Caribbean-South American Plate Boundary and Regional Tectonics*, edited by W. Bonini et al., *Geol. Soc. Am. Mem.*, *162*, 89–121, 1984.

Farley, K. A., J. H. Natland, and H. Craig, Binary mixing of enriched and undegassed (primitive?) mantle components (He, Sr, Nd, Pb) in Samoan lavas, *Earth Planet. Sci. Lett.*, *111*, 183–199, 1992.

Geist, J. D., W. M. White, and A. R. McBirney, Plume-asthenosphere mixing beneath the Galápagos archipelago, *Nature*, *333*, 657–660, 1988.

Graham, D. W., D. M. Christie, K. S. Harpp, and J. E. Lupton, Mantle plume helium in submarine basalts from the Galápagos Platform, *Science*, *262*, 2023–2026, 1993.

Hanan, B. B., and D. W. Graham, Lead and helium isotope evidence from oceanic basalts for a common deep source of mantle plumes, *Science*, *272*, 991–995, 1996.

Hanan, B. B., R. H. Kingsley, and J.-G. Schilling, Migrating ridge - Hotspot Interactions: Pb isotope evidence in the South Atlantic, *Nature*, *322*, 137–144, 1986.

Hanan, B. B., J. Blichert-Toft, R. Kingsley, and J.-G. Schilling, Depleted Iceland mantle plume geochemical signature: Artifact of multicomponent mixing?, *Geochem. Geophys. Geosyst.*, *1*, Paper number 1999GC000009, 2000.

Handschumacher, D. W., Post-Eocene plate tectonics of the eastern Pacific, in *The Geophysics of the Pacific Ocean Basin and Its Margin*, *Geophys. Monogr. Ser.*, vol. 19, edited by G. H. Sutton, M. H. Manghnani, and R. Moberly, pp. 177–202, AGU, Washington, D. C., 1976.

Harpp, K. S., and W. M. White, Tracing a mantle plume: Isotopic and trace element variations of Galápagos seamounts, *Geochem. Geophys. Geosyst.*, *2*, Paper number 2000GC000137, 2001.

Hart, S. R., A large scale isotope anomaly in the Southern Hemisphere mantle, *Nature*, *309*, 753–757, 1984.

Hart, S. R., E. H. Hauri, L. A. Oschmann, and J. A. Whitehead, Mantle plumes and entrainment: Isotopic evidence, *Science*, *256*, 517–520, 1992.

Hauff, F., K. Hoernle, H.-U. Schmincke, and R. Werner, A Mid cretaceous origin for the Galápagos hotspot: Volcanological, petrological, and geochemical evidence from Costa Rican oceanic crustal segments, *Geol. Rundschau*, *86*, 141–155, 1997.

Hauff, F., K. Hoernle, P. v. d. Bogaard, G. Alvarado, and D. und Garbe-Schönberg, Age and geochemsitry of basaltic complexes in western Costa Rica: Contributions to the geo-

tectonic evolution of Central America, *Geochem. Geophys. Geosyst.*, *1*, Paper number 1999GC000020, 2000a.

Hauff, F., K. Hoernle, G. Tilton, D. Graham, and A. C. Kerr, Large volume recycling of oceanic lithosphere over short time scales: Geochemical constraints from the Caribbean Large Igneous Province, *Earth Planet. Sci. Lett.*, *174*, 247–263, 2000b.

Hauff, F., R. Werner, D. M. Christie, and K. Hoernle, Morphological and Sr-Nd-Pb isotope variations along the Cocos-Nazca Spreading Center (CNS) from 85°W to 92.5°W, *Eur. J. Mineral.*, *14*, 64, 2002.

Hey, R., F. K. Duennebier, and W. J. Morgan, Propagating rifts on Midocean Ridges, *J. Geophys. Res.*, *85*, 3647–3658, 1980.

Hoernle, K., R. Werner, J. P. Morgan, J. Bryce, and J. Mrazek, Existence of complex spatial zonation in the Galápagos Plume for at least 14 m. y., *Geology*, *28*, 435–438, 2000.

Hoernle, K., P. V. d. Bogaard, R. Werner, B. Lissinna, F. Hauff, G. Alvarado, and D. Garbe-Schönberg, Missing history (16–71 Ma) of the Galápagos Hotspot: Implications for the tectonic and biological evolution of the Americas, *Geology*, *30*, 795–798, 2002a.

Hoernle, K., G. Tilton, M. J. Le Bas, S. Duggen, and D. Garbe-Schönberg, Geochemistry of oceanic carbonatites compared with continental carbonatites: Mantle recycling of oceanic crustal carbonate, *Contrib. Mineral. Petrol.*, *142*, 520–542, 2002b.

Ionov, D., Trace element composition of mantle-derived carbonates and coexisting phases in peridotite xenoliths from alkali basalts, *J. Petrol.*, *39*, 1931–1941, 1998.

Kerr, A. C., J. Tarney, G. F. Marriner, G. T. Klaver, A. D. Saunders, and M. F. Thirlwall, The geochemistry and petrogenesis of the late-Cretaceous picrites and basalts of Curaçao, Netherlands Antilles: A remnant of an oceanic plateau, *Contrib. Mineral. Petrol.*, *124*, 29–43, 1996.

Kerr, A. C., J. Tarney, G. F. Marriner, A. Nivia, and A. D. Saunders, The Caribbean-Colombian Igneous Province: The internal anatomy of an oceanic plateau, in *Large Igneous Provinces*, *Geophys. Monogr. Ser.*, vol. 100, edited by J. Mahoney and M. F. Coffin, pp. 123–144, AGU, Washington, D. C., 1997a.

Kerr, A. C., G. F. Marriner, J. Tarney, A. Nivia, A. D. Saundrs, M. F. Thirlwall, and C. W. Sinton, Cretaceous basaltic terranes in Western Colombia: Elemental, chronological and Sr-Nd isotopic constraints on petrogenesis, *J. Petrol.*, *38*, 677–702, 1997b.

Kerr, A. C., J. Tarney, P. D. Kempton, P. Spadea, A. Nivia, G. F. Marriner, and R. A. Duncan, Pervasive mantle plume head heterogeneity: Evidence from the late Cretaceous Caribbean-Colombian oceanic plateau, *J. Geophys. Res.*, *107*(B7), 2140, doi:10.1029/2001JB000790, 2002.

Kurz, M. D., and D. J. Geist, Dynamics of the Galápagos hotspot from helium isotope gechemistry, *Geochim. Cosmochim. Acta*, *63*, 4139–4156, 1999.

Meschede, M., U. Barckhausen, and H.-U. Worm, Extinct spreading on the Cocos Ridge, *Terra Nova*, *10*, 211–216, 1998.

Patchett, P. J., W. M. White, H. Feldmann, S. Kielinczuk, and A. W. Hofmann, Hafnium/rare earth element fractionation in the sedimentary system and crustal recycling into the Earth's mantle, *Earth Planet. Sci. Lett.*, *69*, 365–378, 1984.

Pindel, J. L., and S. F. Barrett, Geological Evolution of the Caribbean region, a plate tectonic perspective, in The Caribbean Region, *Geol. Soc. Am.*, 405–432, 1990.

Planck, T., and C. H. Langmuir, The chemical composition of subducting sediment and it's consequences for the crust and mantle, *Chem. Geol.*, *145*, 325–394, 1998.

Richards, M. A., R. A. Duncan, and V. E. Courtillot, Flood basalts and hotspot tracks: Plume heads and tails, *Science*, *246*, 103–107, 1989.

Salters, V. J. M., and S. R. Hart, The hafnium paradox and the role of garnet in the source of mid-ocean-ridge basalts, *Nature*, *342*, 420–422, 1989.

Salters, V. J. M., and S. R. Hart, The mantle source of ocean ridges, islands and arcs: The Hf isotope connection, *Earth Planet. Sci. Lett.*, *104*, 364–380, 1991.

Sinton, C. W., R. A. Duncan, and P. Denyer, Nicoya Peninsula, Costa Rica: A single suite of Caribbean oceanic plateau magmas, *J. Geophys. Res.*, *102*, 15,507–15,520, 1997.

Sinton, C. W., R. A. Duncan, M. Storey, J. Lewis, and J. J. Estrada, An oceanic flood basalt province within the Caribbean plate, *Earth Planet. Sci. Lett.*, *155*, 221–235, 1998.

Sun, S. S., and W. F. McDonough, Chemical and isotopic systematics of oceanic basalts: Implications for mantle composition and processes, in *Magmatism in the Ocean Basins*, *Spec. Publ. Geol. Soc. Am.*, *42*, 313–345, 1989.

Toomey, D. R., E. E. E. Hooft Toomey, S. C. Solomon, D. E. James, and M. L. Hall, Upper mantle structure beneath the Galápagos archipelago from body wave data (abstract), *Eos Trans. AGU*, *82*(47), Fall Meet. Suppl., Abstract T41D-04, 2001.

Vervoort, J. D., P. J. Patchett, J. Blichert-Toft, and F. Albarède, Relationships between Lu-Hf and Sm-Nd isotopic systems in the global sedimentary system, *Earth Planet. Sci. Lett.*, *168*, 79–99, 1999.

Werner, R., K. Hoernle, P. v. d. Bogaard, C. Ranero, R. v. Huene, and D. Korich, A drowned 14 Ma old Galápagos Archipelago off the coast of Costa Rica: Implications for evolutionary and tectonic models, *Geology*, *27*, 499–502, 1999 .

White, W. M., and A. W. Hofmann, Geochemistry of the Gálapagos Islands: Implications for mantle dynamics and evolution, *Yearbook Carnegie Inst.*, *77*, 596–606, 1978.

White, W. M., A. R. McBirney, and R. A. Duncan, Petrology and geochemistry of the Galápagos Islands: Portrait of a pathological mantle plume, *J. Geophys. Res.*, *98*, 19,533–19,563, 1993.

Wilson, D. S., and R. N. Hey, History of rift propagation and magnetization intensity for the Cocos-Nazca spreading center, *J. Geophys. Res.*, *100*, 10,041–10,056, 1995.